第一届“粤港澳”核物理论坛
广东 珠海，2022年7月2-6日

月球及行星辐射环境研究

张小平

xpzhang@must.edu.mo

澳门科技大学月球与行星科学国家重点实验室

提纲

1. 研究背景介绍
2. 空间粒子的时空变化特征
3. 宇宙线与月球及火星表面相互作用
4. 结论

Energetic Particles in the Heliosphere

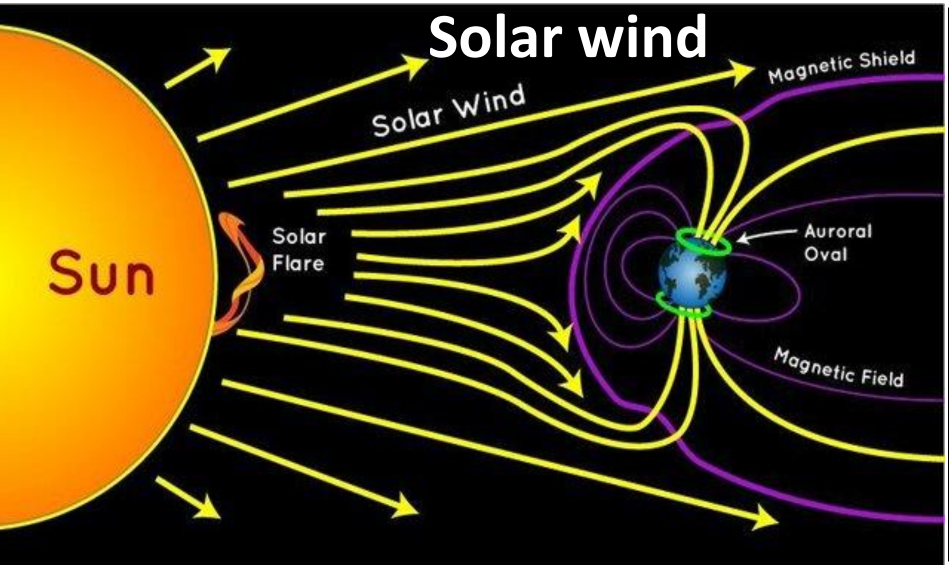

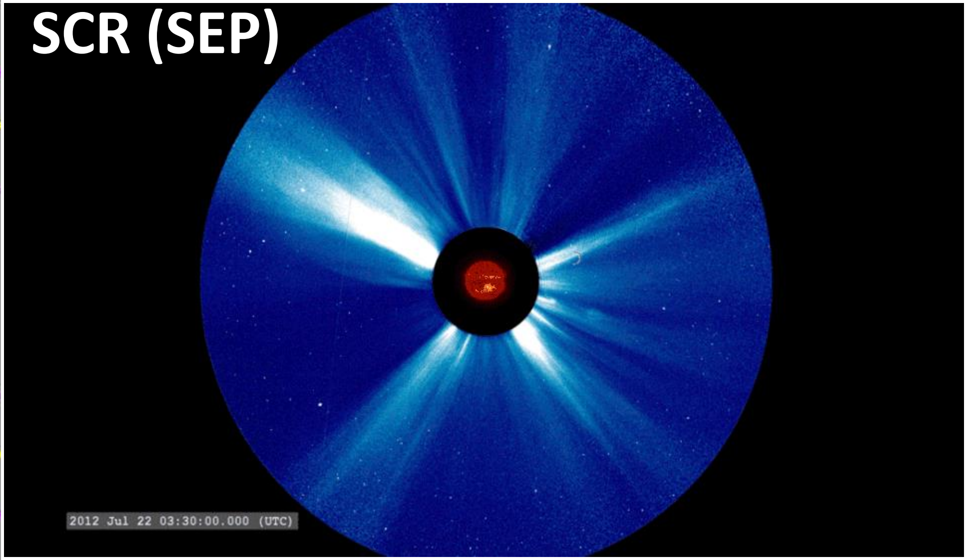

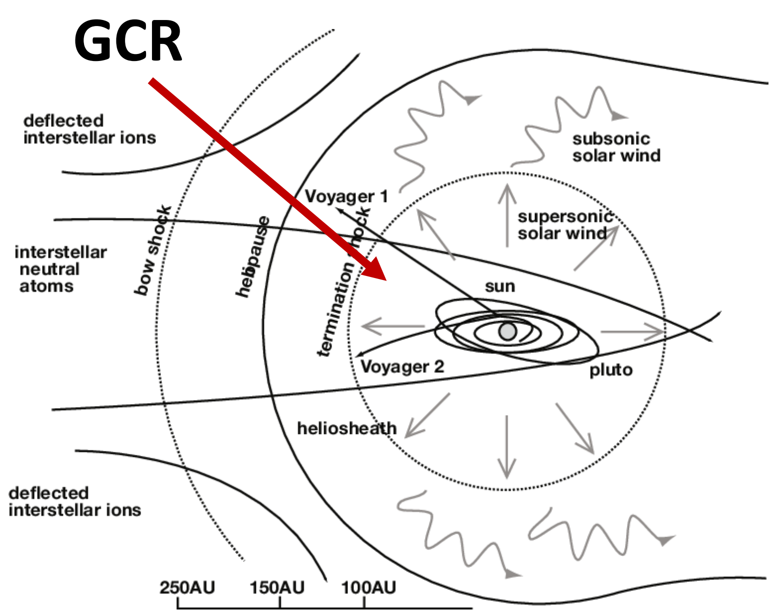

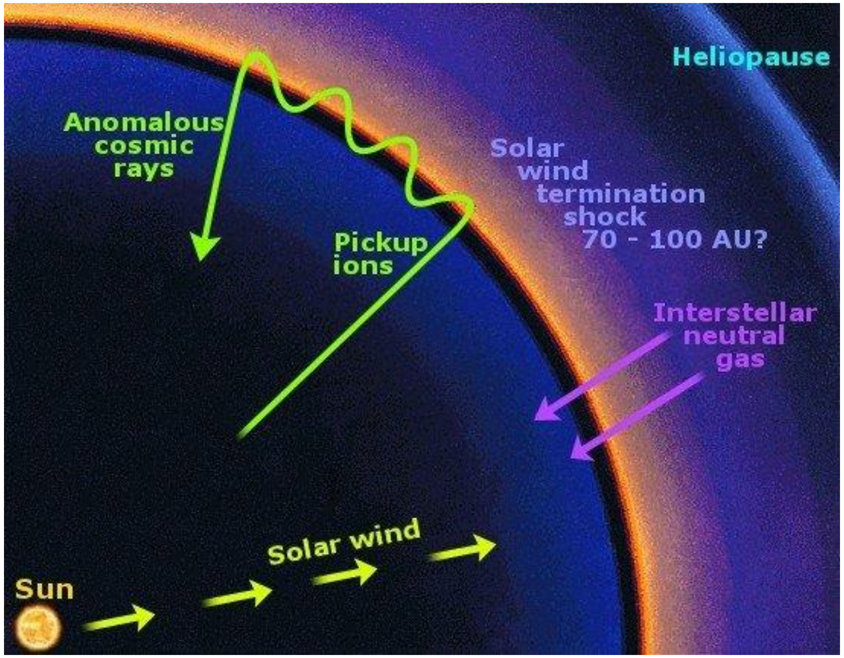

ACR

• Introduction

Radiation environment in the inner solar system：

	Main Particle types	Proton flux ($cm^{-2}s^{-1}$)	Energy	Chief effects on the Moon
Solar Wind	e^- p α	~$3x10^8$	1.5-10 KeV	(1) Inject into the lunar surface, (300nm) (2) Charge the lunar surface，influence the float of lunar dust
Solar Cosmic Rays (SCR)	p	~100	1-200 MeV	(1) Produce the radioactive nuclides (such as ^{26}Al, ^{53}Mn) (<10 cm)
Galactic Cosmic Rays (GCR)	p ~93% α ~ 6%	1~7	0.01-10^5 GeV	(1)Produce the radioactive nuclides (2)Produce the stable nuclides (such as ^{21}N, ^{15}N) (0-10 m)
Anomalous cosmic rays (ACR)	He, N, O, Ne, Ar	~0.01-1	~5–50 $MeVnuc^{-1}$	(1) Produce the radioactive nuclides (such as ^{26}Al, ^{53}Mn) (<10 cm)

2、空间粒子的时空变化特征

Particle filling effect in the lunar wake

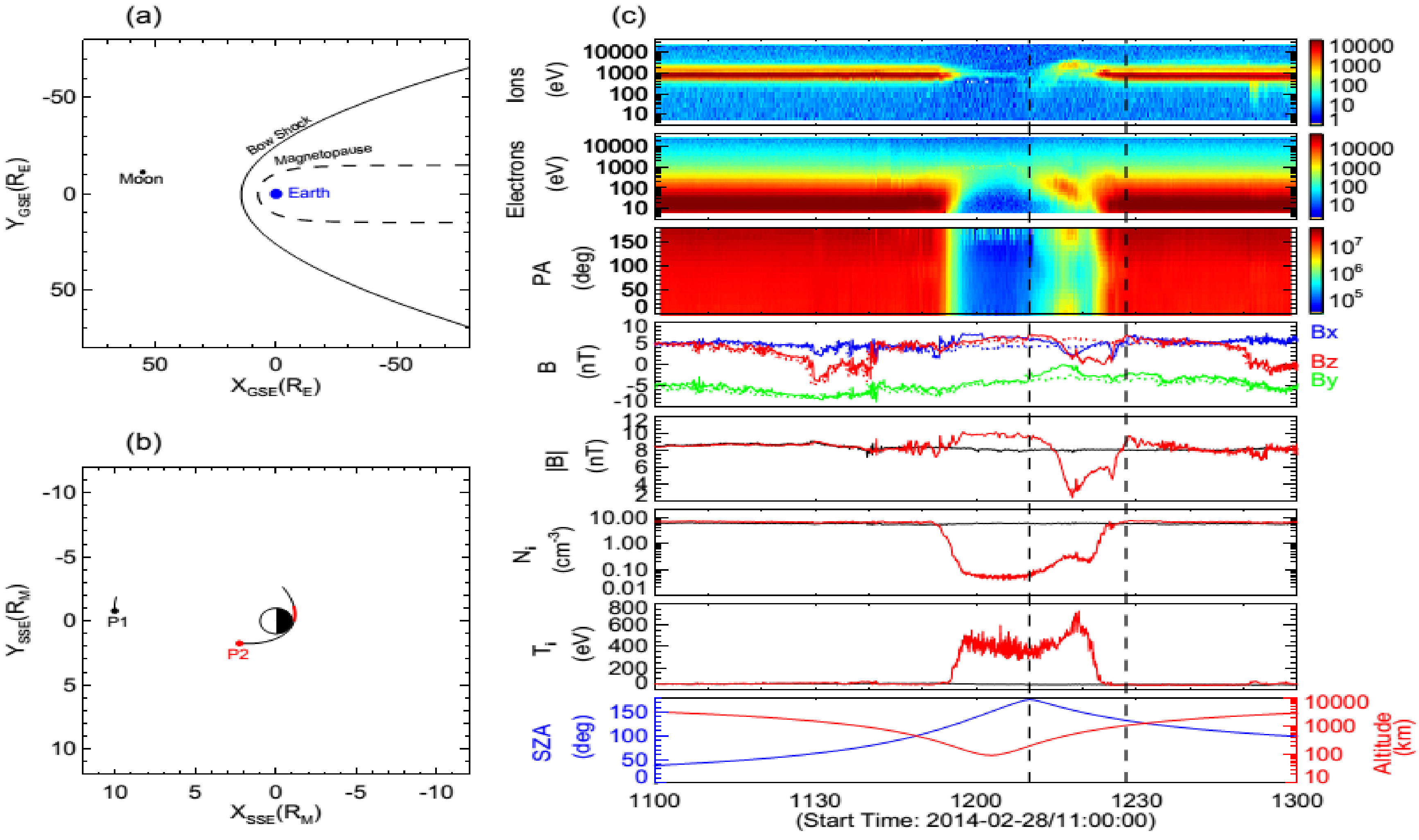

Guo, ZHANG et al., APJ 2016

Diamagnetic hole in the lunar wake

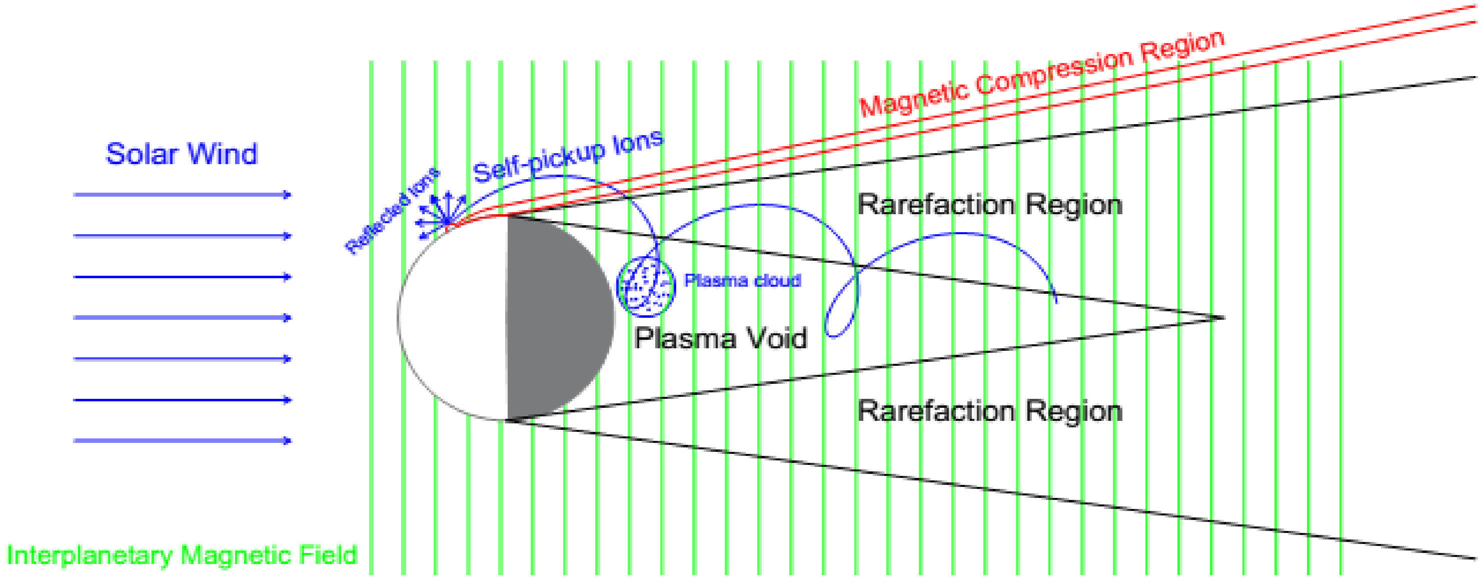

- ✓ Up to 7% of the incident solar wind particles are reflected back by the magnetic anomaly region and picked up into the lunar wake (about 1% in previous observation)
- ✓ **"Diamagnetic hole"** observed for the first time as massive particles gather in lunar wake

GCR intensities in the solar minimum 24/25 (2019-2020)

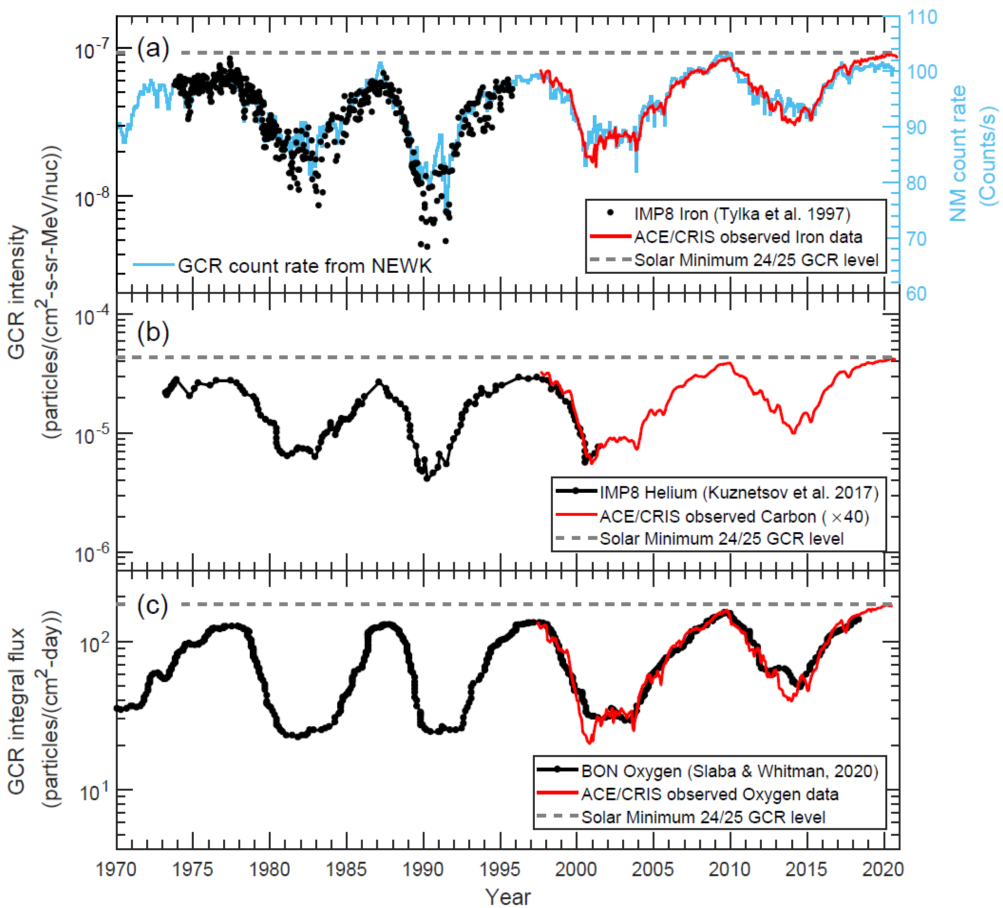

- ✓ ACE satellite: Sun-Earth L1 Lagrange point
- ✓ **Record-breaking GCR intensities since space era**
- ✓ The peak ground-based neutron monitors (NM) count rates in 2019-2020 are lower than those in late 2009

Fu, ZHANG et al., 2021, ApJS

Variation of sunspot numbers

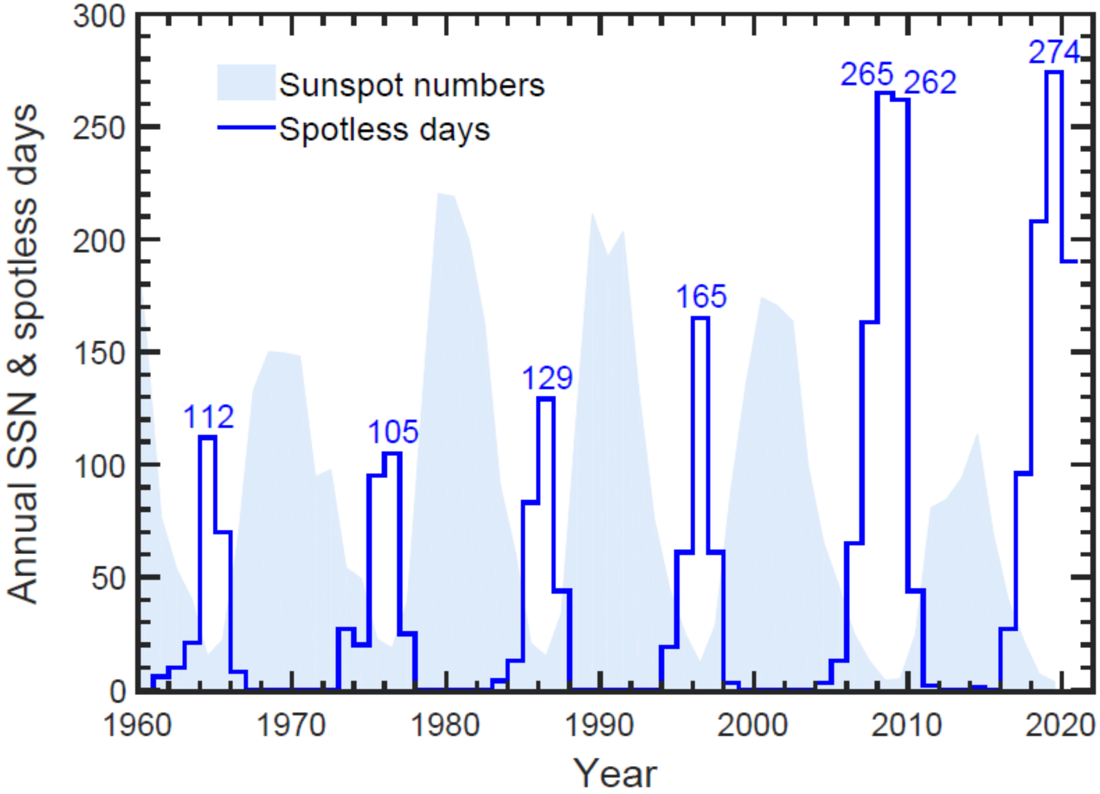

- ✓ Totally 274 days without sunspots in the year 2019, the most in the past 107 years
- ✓ **Extraordinarily quiet solar activity**

Fu, ZHANG et al., 2021, ApJS

Solar wind/interplanetary parameters

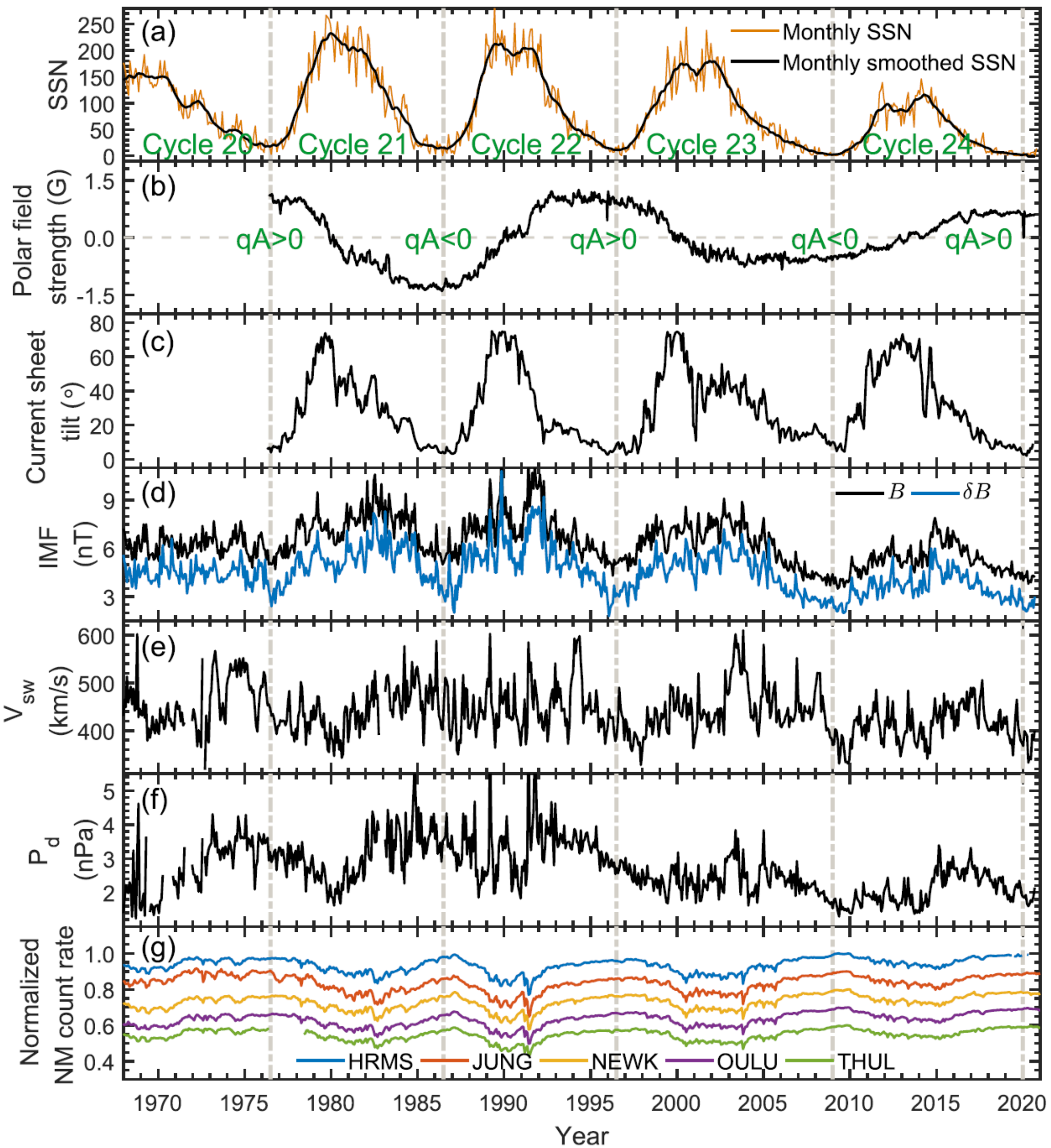

GCR spectra

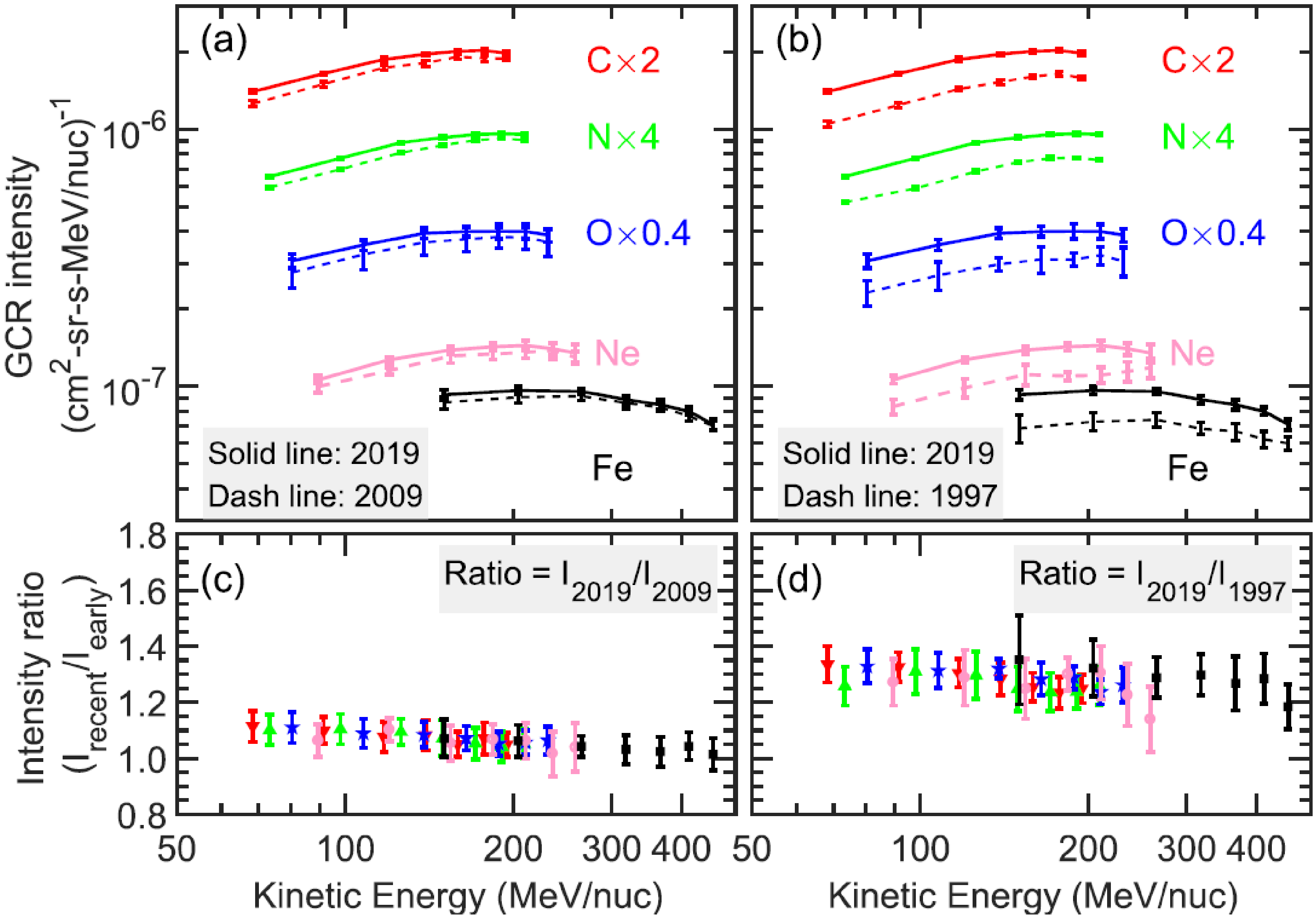

(a)
(b)
C×2
N×4
O×0.4
Ne
Fe
Solid line: 2019
Dash line: 2009
Solid line: 2019
Dash line: 1997
GCR intensity
(cm^2-sr-s-MeV/nuc)$^{-1}$
10^{-6}
10^{-7}
(c)
(d)
Ratio = I$_{2019}$/I$_{2009}$
Ratio = I$_{2019}$/I$_{1997}$
Intensity ratio
(I$_{recent}$/I$_{early}$)
1.8
1.6
1.4
1.2
1.0
0.8
50
100
200
300 400
Kinetic Energy (MeV/nuc)
Kinetic Energy (MeV/nuc)

GCR radiation dose rates on the lunar surface

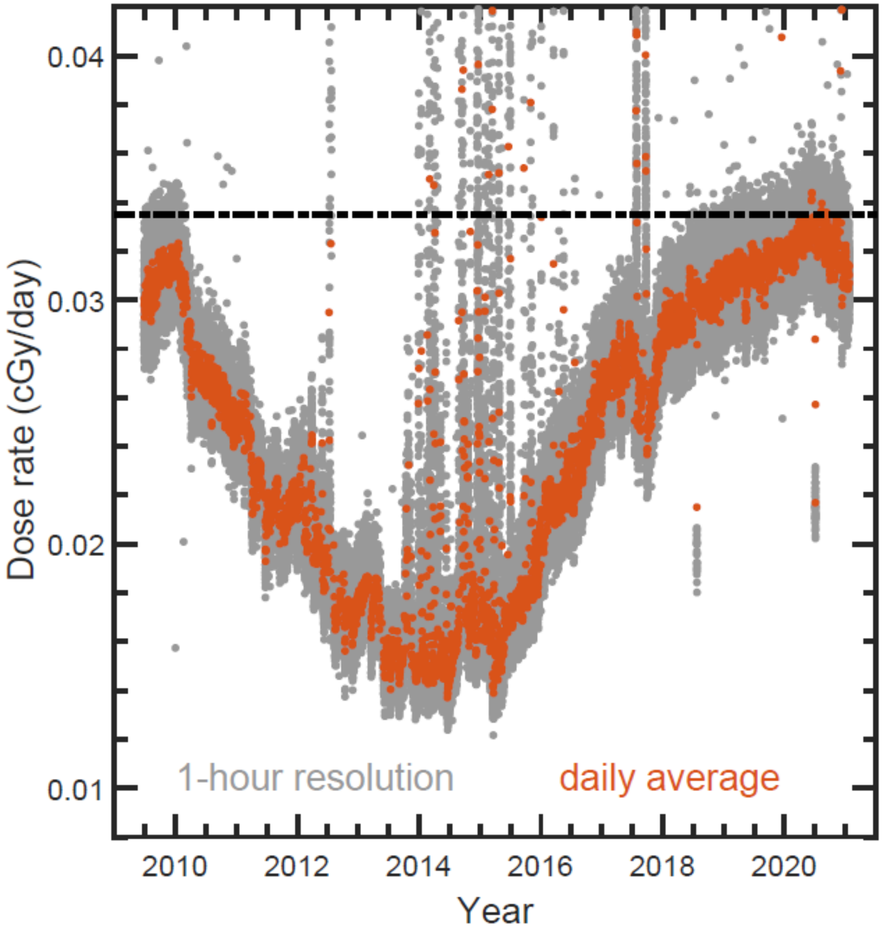

- ✓ LRO/CRaTER data
- ✓ **Peak value of dose rates in the first half of 2020 is ~5% higher than that in 2009-2010**
- ✓ May be the highest dose rates on the lunar surface since the 1980s, raise higher requirements for radiation shielding and protection

ACR-GCR transition energy

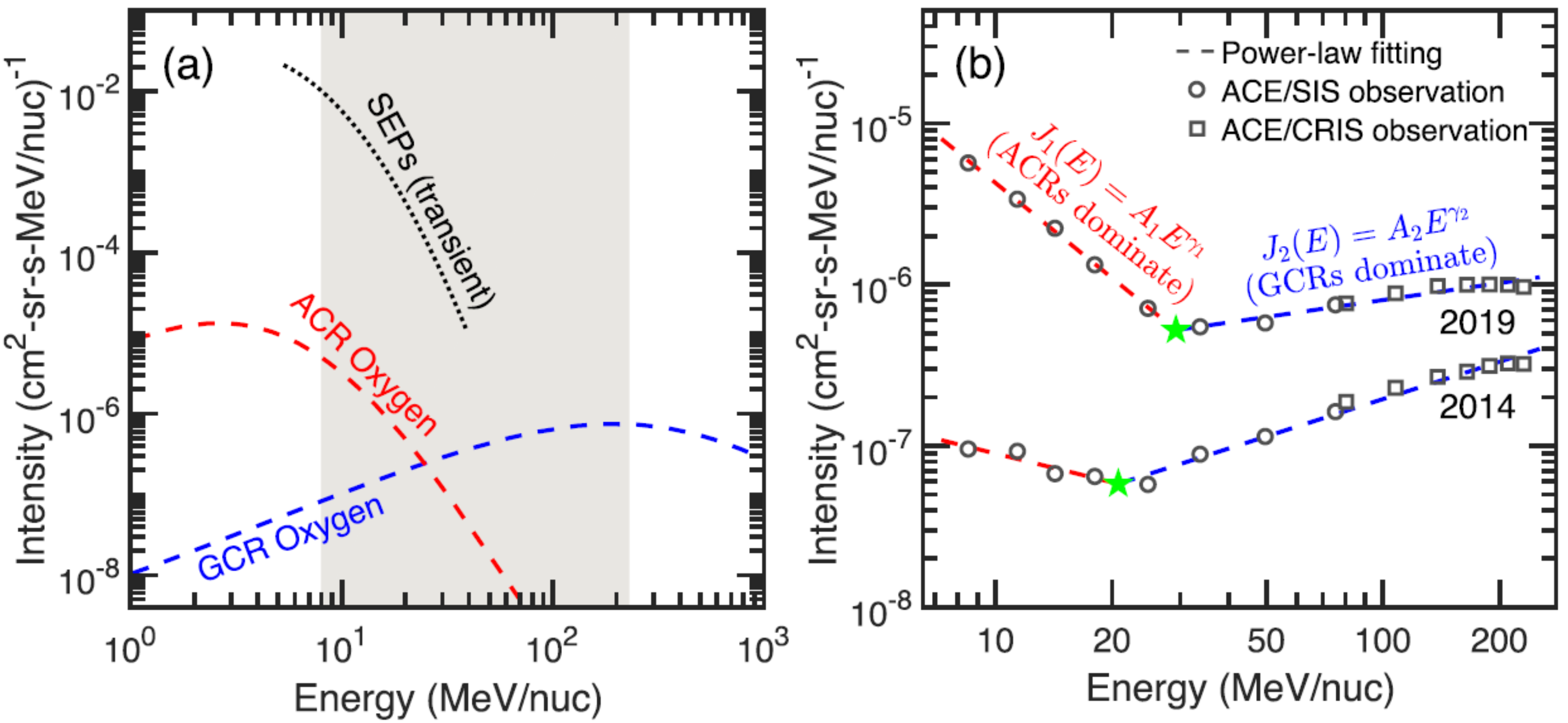

Fu, Zhao, ZHANG et al., 2021, ApJL

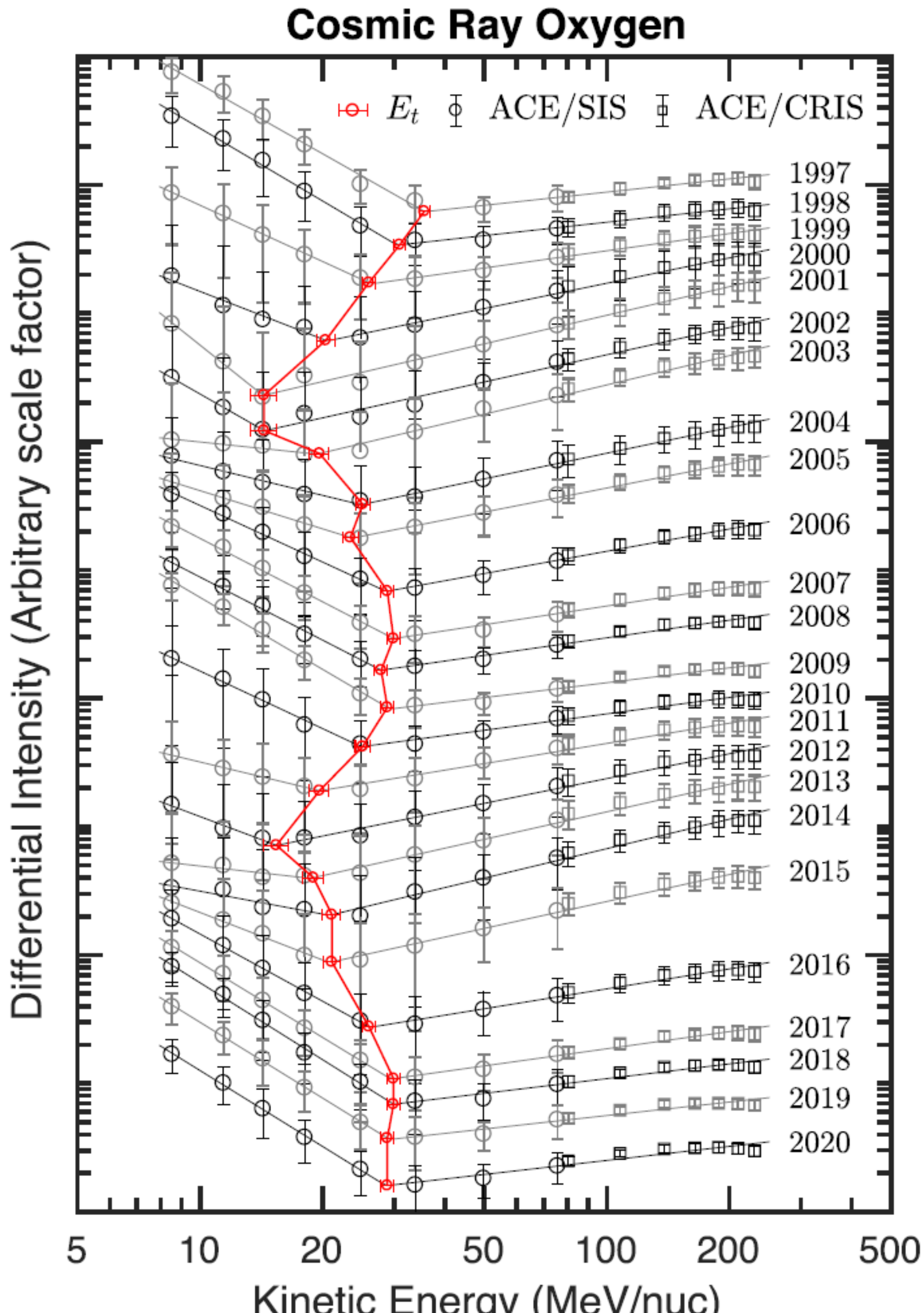

Cosmic Ray Oxygen
E_t
ACE/SIS
ACE/CRIS
1997
1998
1999
2000
2001
2002
2003
2004
2005
2006
2007
2008
2009
2010
2011
2012
2013
2014
2015
2016
2017
2018
2019
2020
Differential Intensity (Arbitrary scale factor)
5
10
20
50
100
200
500
Kinetic Energy (MeV/nuc)

Solar modulation on ACR and GCR transition energies

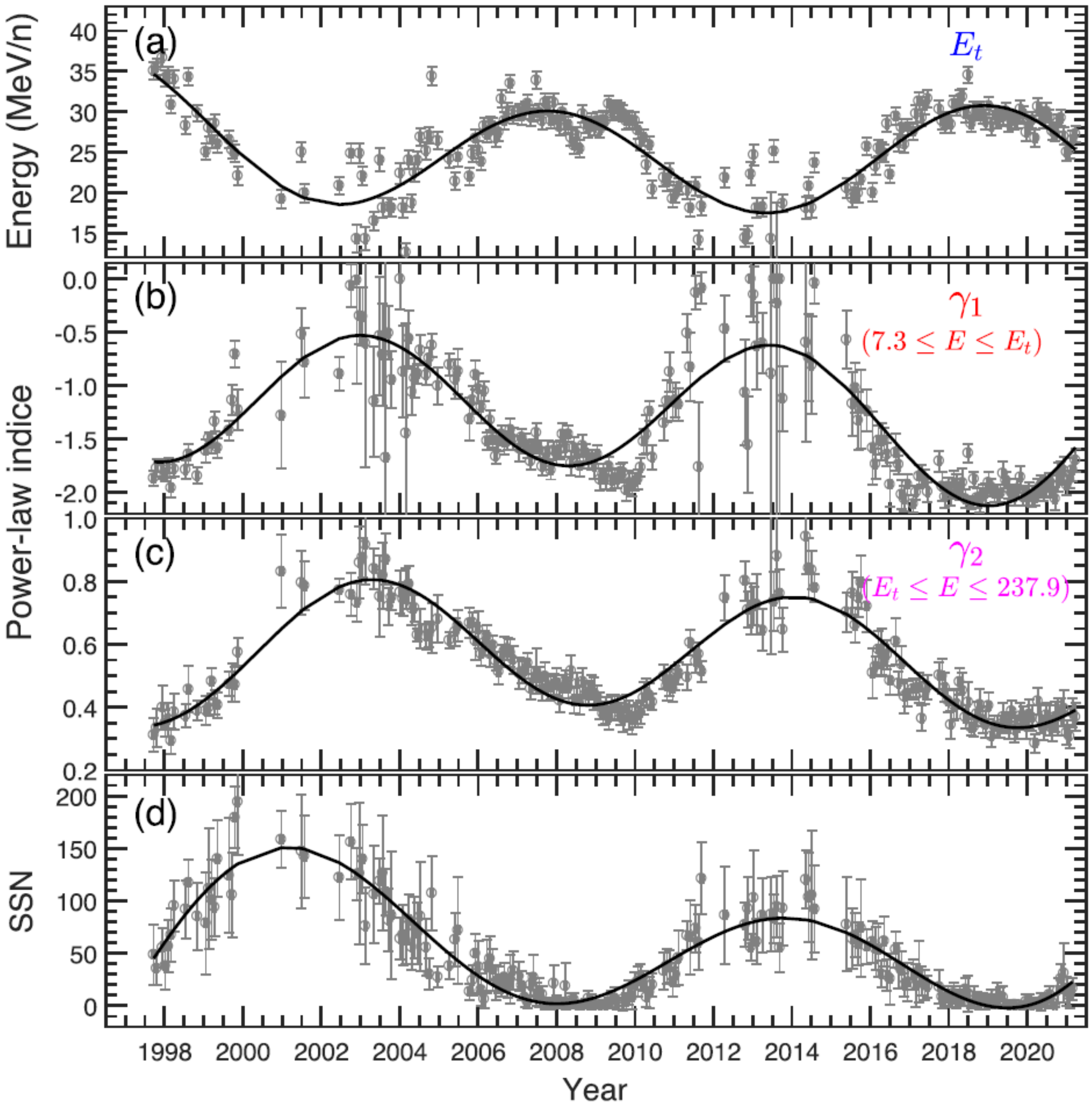

Fu, Zhao, ZHANG et al., 2021, ApJL

ACR intensities did not reach maximum in 2019-2020

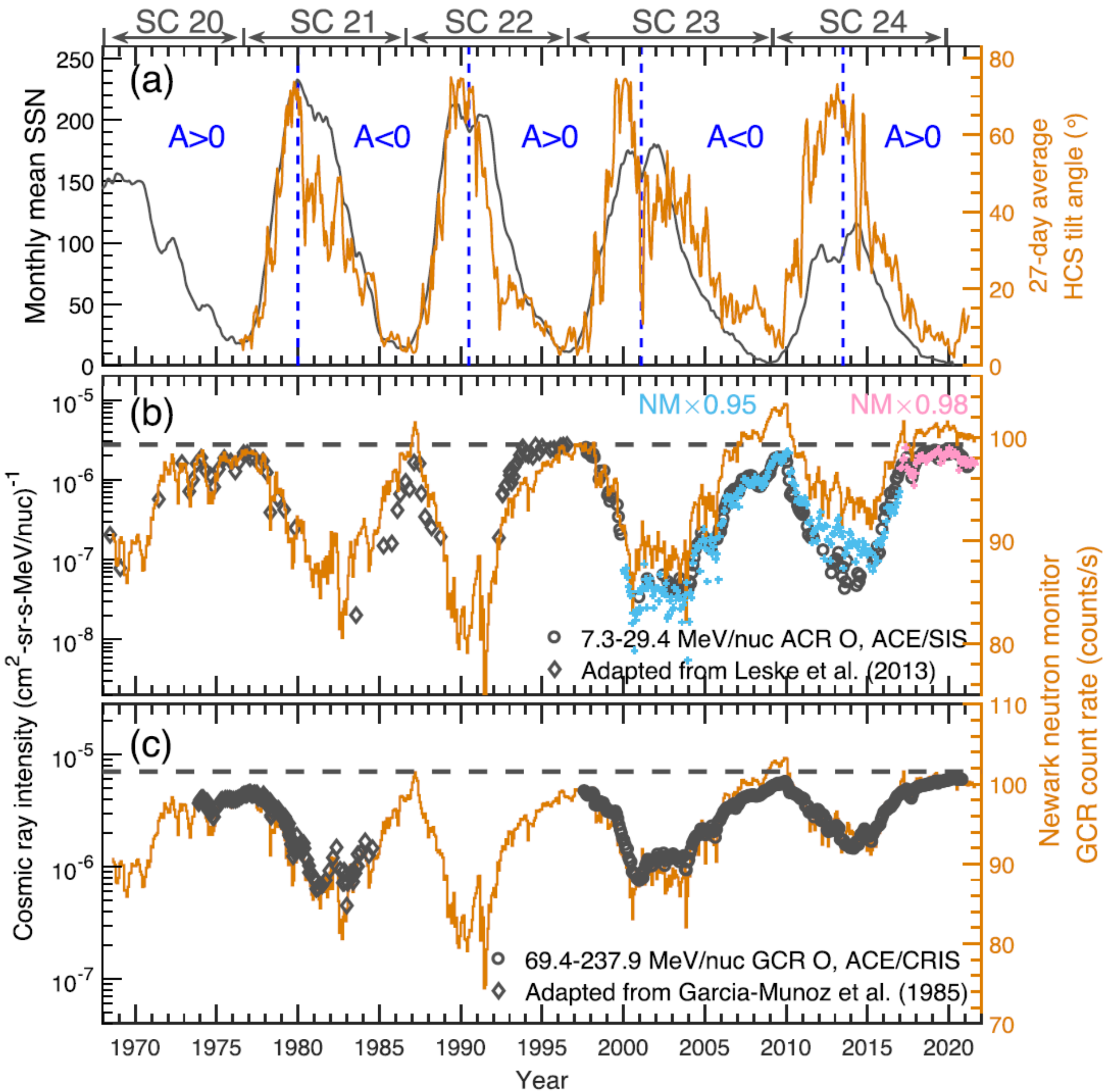

ACR intensities follows more closely with HCS tilt angle

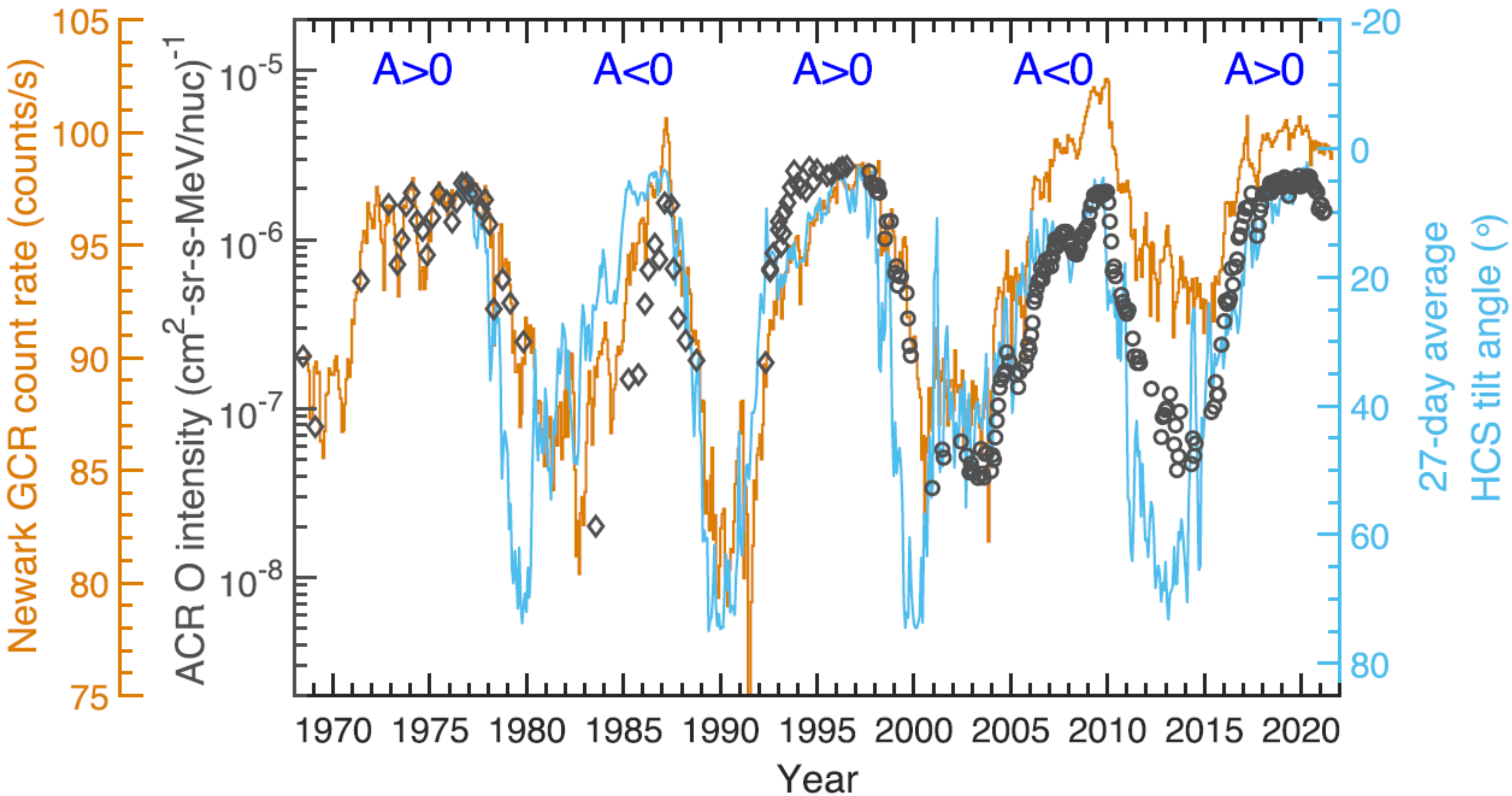

Current sheet drift may play an important role in ACR modulation
(Leske et al. 2013)

First measurements of low-energy cosmic rays on the surface of the lunar farside

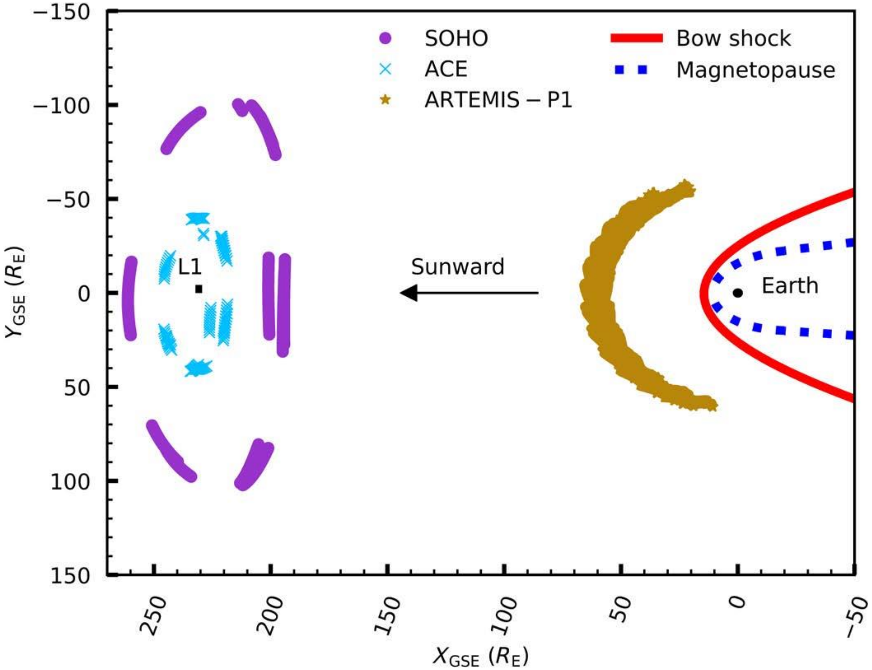

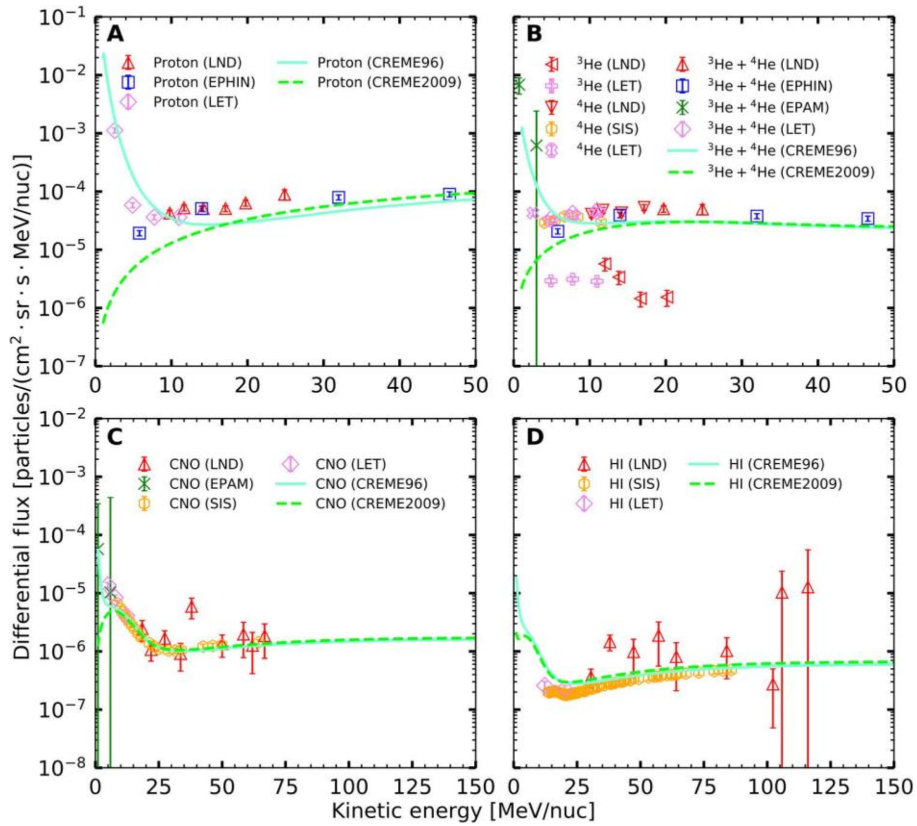

Luo, ZHANG et al., 2022, Science Advances

First measurements of low-energy cosmic rays on the surface of the lunar farside

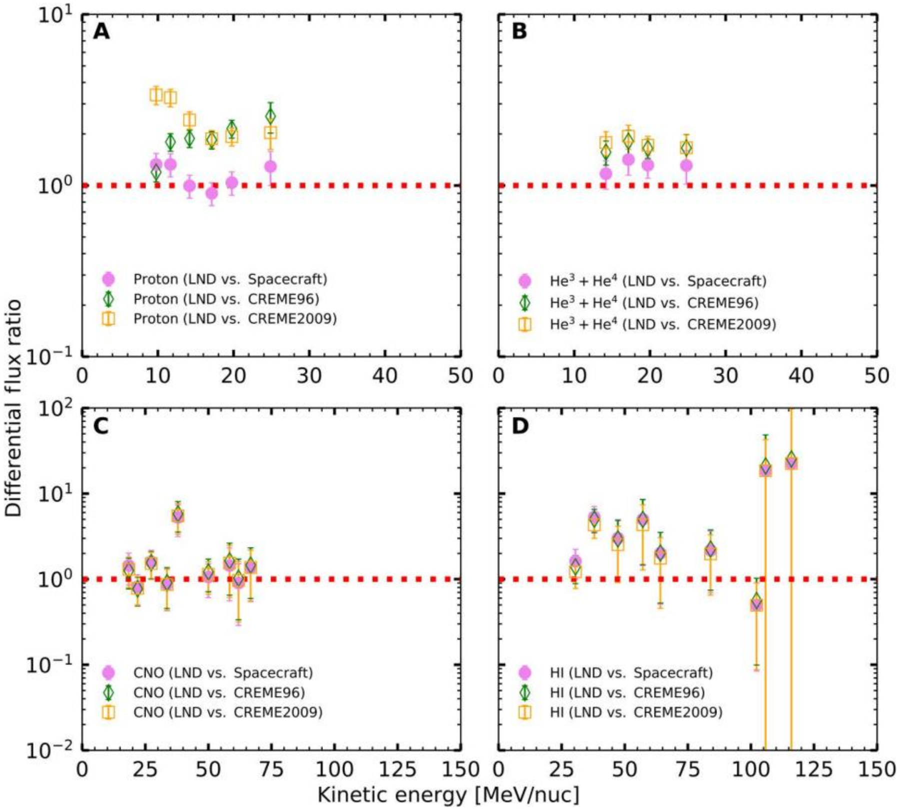

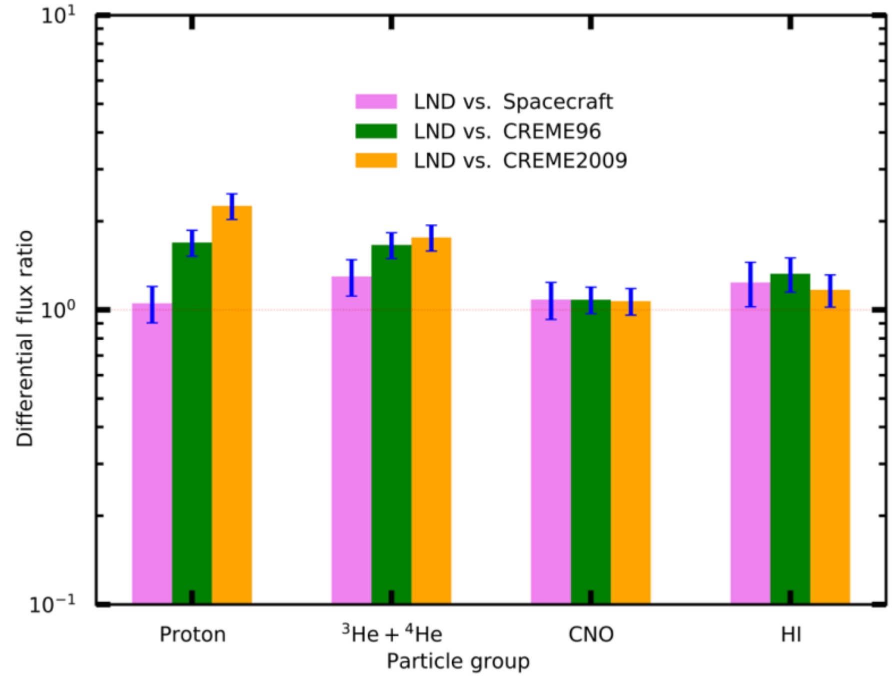

Luo, ZHANG et al., 2022, Science Advances

3. 宇宙线与月球及火星表面相互作用

空间辐射环境

月球　无大气，无磁场

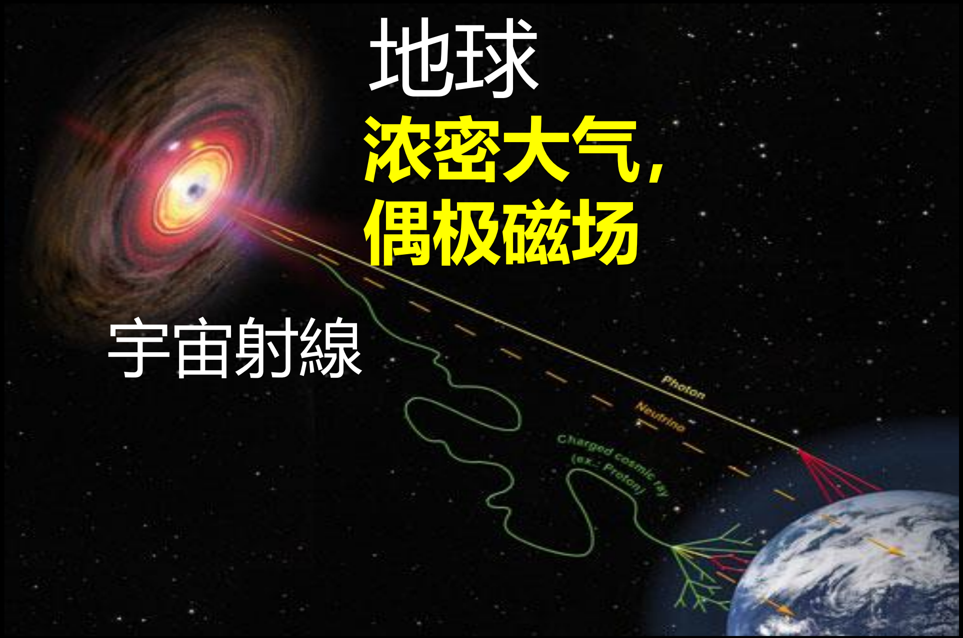

地球
浓密大气，
偶极磁场

宇宙射線

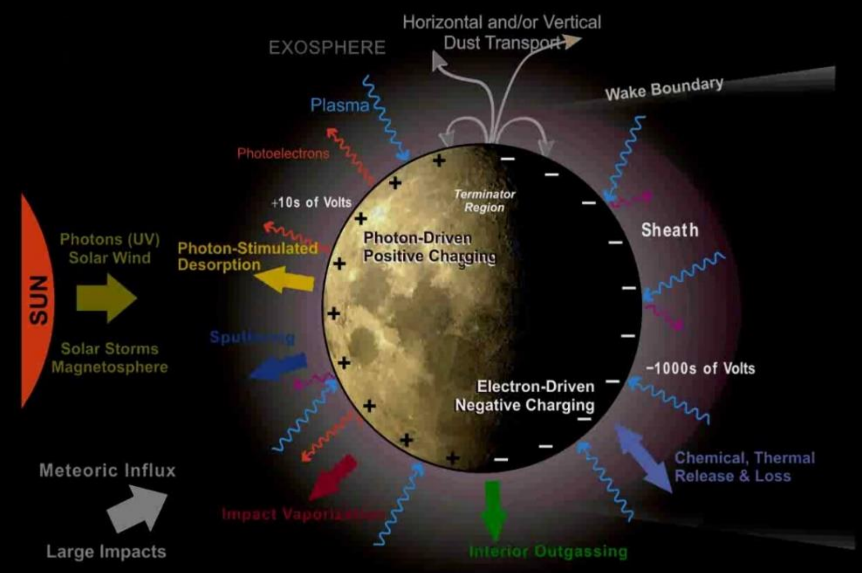

火星　稀薄大气，区域磁场

月球、火星和地球的辐射环境迥异

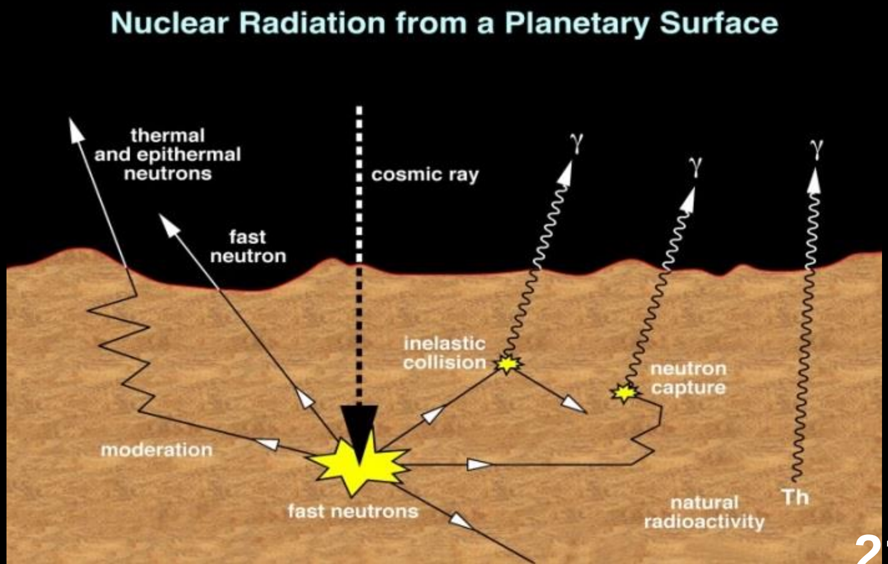

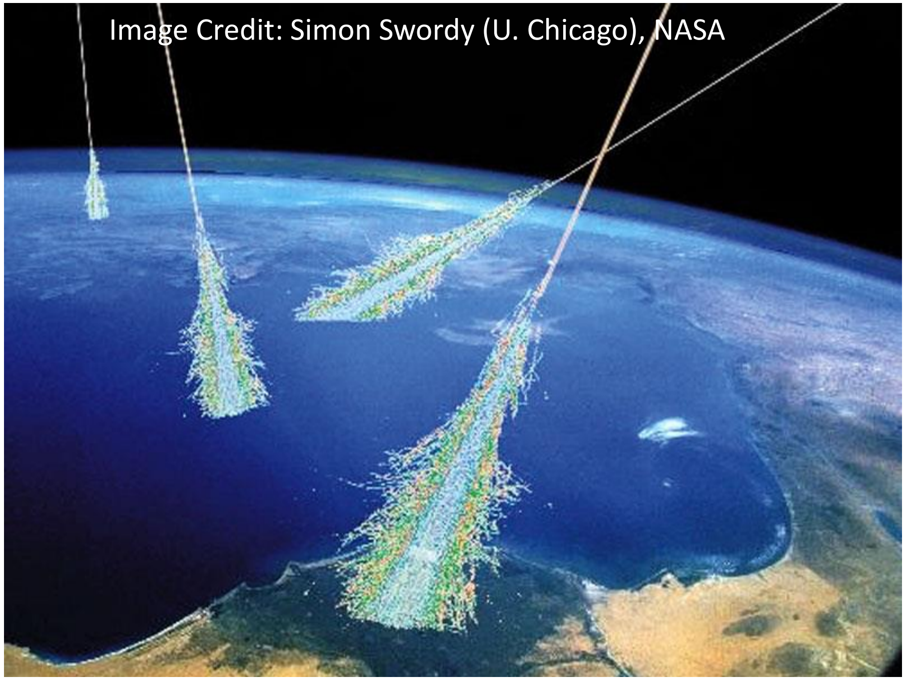

Showers of energetic cosmic rays in the Earth's atmosphere

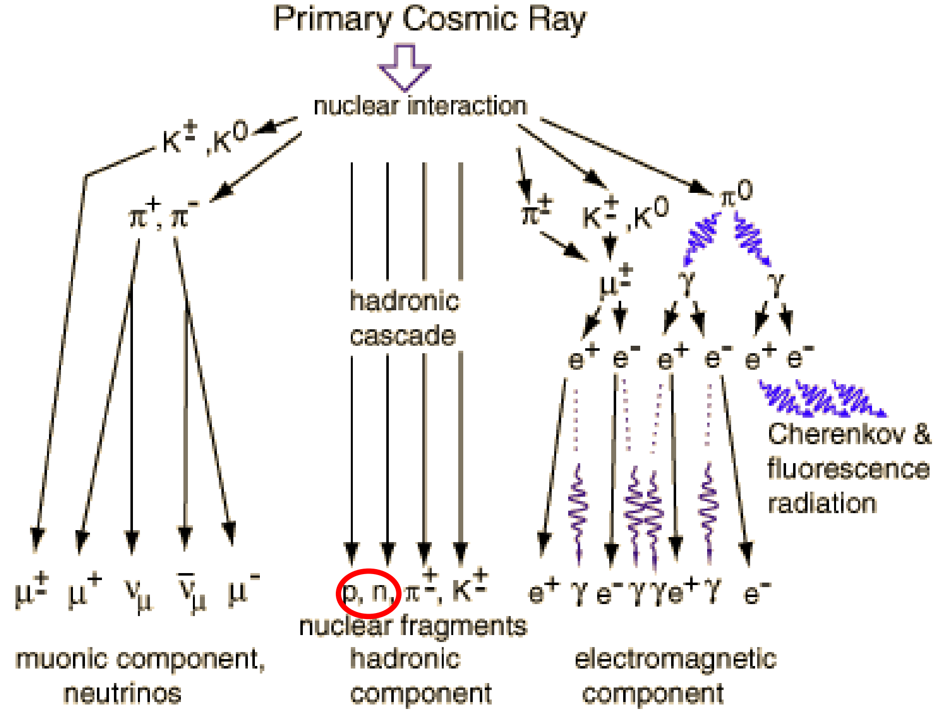

+ N

N(n,x)N'
N(p,x)N'

Cosmogenic Nuclides (N')

^{3}He, ^{10}Be , ^{14}C, ^{21}Ne, ^{22}Na, ^{36}Cl, ^{38}Ar, ^{40}K, ^{53}Mn, ^{60}Co et al

Half-life (5×10^{3} - 5×10^{6} a) < Exposure age(10^{7} a)

传统计算方法

- In the previous work by Reedy and Arnold [1972], Masarik and Reedy [1994], Kim [2010] and Dong[2014].

GCR particles + Soil

- protons
  - P + O —> ^{10}Be+X
  - P +Mg—>^{10}Be+X
  - P + Al—>^{10}Be+X
  - P + Si—>^{10}Be+X
  - P + Fe—>^{10}Be+X
- neutrons
  - n + O—>^{10}Be+X
  - n + Si—>^{10}Be+X

^{10}Be production

传统计算方法

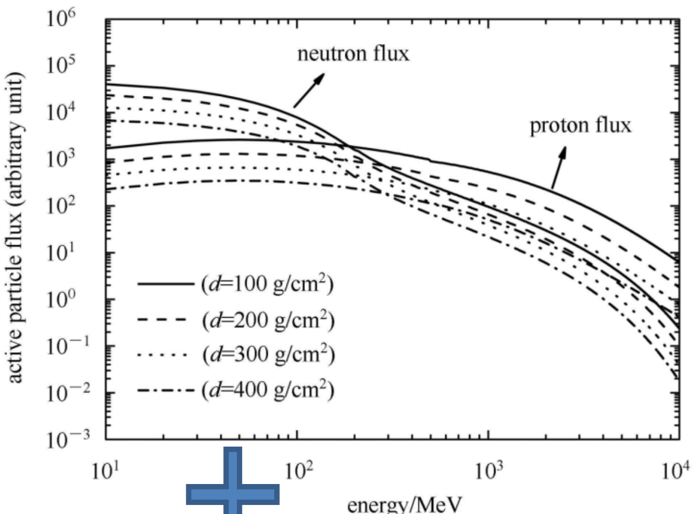
neutron flux
proton flux
active particle flux (arbitrary unit)
energy/MeV
(d=100 g/cm²)
(d=200 g/cm²)
(d=300 g/cm²)
(d=400 g/cm²)

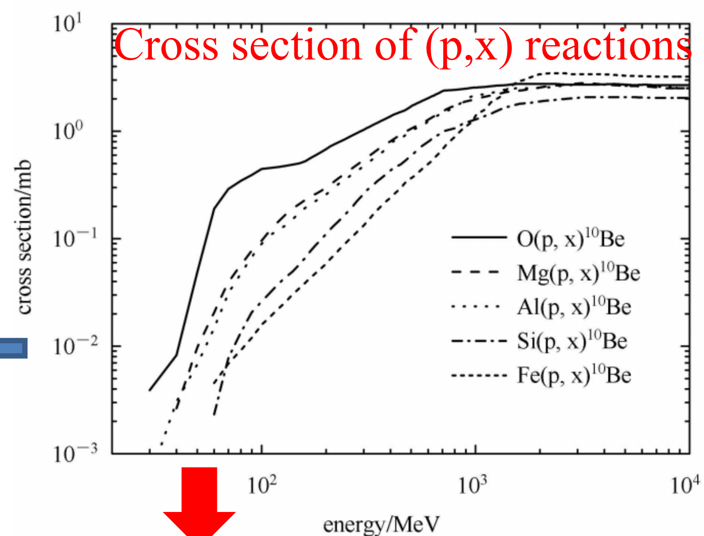
Cross section of (p,x) reactions
cross section/mb
energy/MeV
O(p, x)¹⁰Be
Mg(p, x)¹⁰Be
Al(p, x)¹⁰Be
Si(p, x)¹⁰Be
Fe(p, x)¹⁰Be

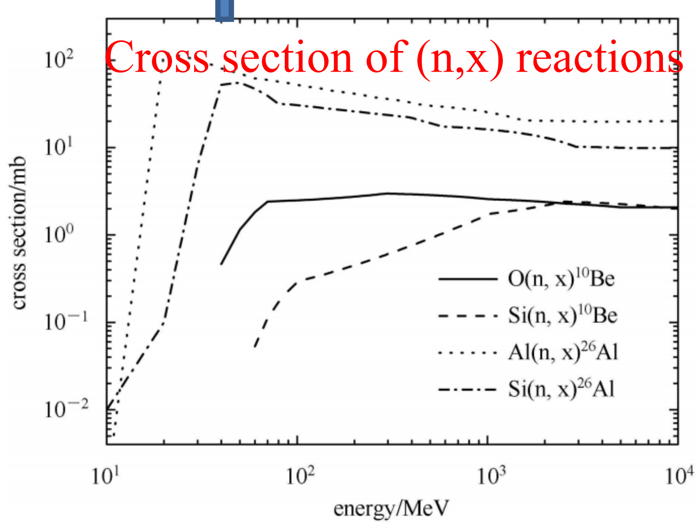
Cross section of (n,x) reactions
cross section/mb
energy/MeV
O(n, x)¹⁰Be
Si(n, x)¹⁰Be
Al(n, x)²⁶Al
Si(n, x)²⁶Al

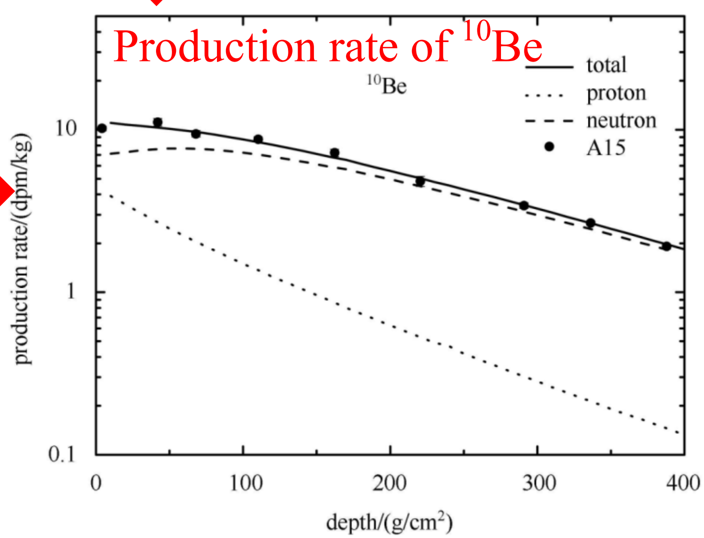
Production rate of ¹⁰Be
¹⁰Be
total
proton
neutron
A15
production rate/(dpm/kg)
depth/(g/cm²)

传统计算方法

Effective GCR fluxes(proton $cm^{-2}s^{-1}$)
for the two model used in MCNPX

Model Nuclide	Apollo 15 drill core	
	BER	CEM
^{10}Be	4.8	4.56
^{26}Al	3.68	3.28
^{14}C	5.08	4.52

存在的问题：模型不自洽，不同的宇宙成因核素，所用的入射宇宙射线通量不同。

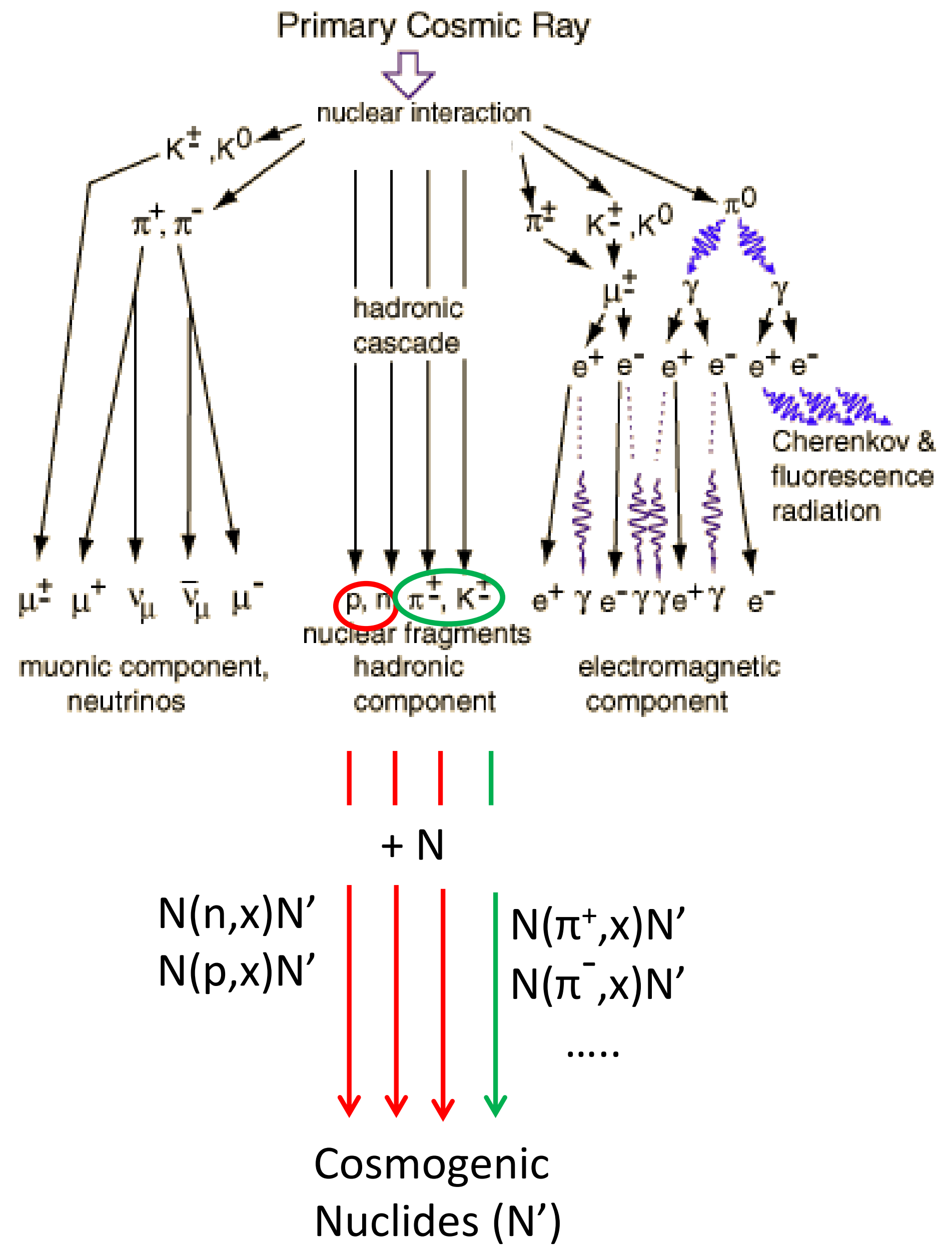

新方法: 计入所有次级粒子的贡献

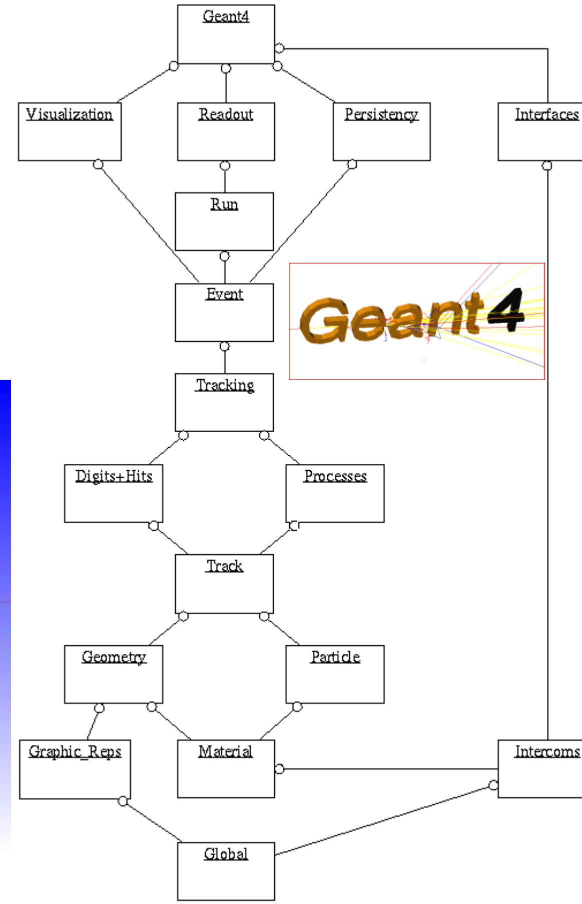

[*Agostinelli et al.*, 2003]

- Method

- **The main parameters of our model:**

➢ The component of the lunar soil:

SiO_2 (46.4%) , TiO_2 (1.83%) , Al_2O_3 (10.8%) , FeO (18.7%) , MnO (0.23%) , MgO (11.5%), CaO (8.5%) , Na_2O (0.4%) , K_2O (0.3%)

Drived from Apollo 15 deep core [Gold et al. 1977]

➢ The physicslist :

G4HadronElasticPhysicsHP

G4HadronPhysicsQGSP_BIC_HP

G4IonElasticPhysics

G4IonBinaryCascadePhysics

G4EmStandardPhysics

G4DecayPhysics

G4RadioactiveDecayPhysics

• Method

➢ The particle source (GCR particles) :

Differential GCR spectra：

$$J_i(T,\Phi) = J_{LIS,i}(T+\Phi_i)\frac{T(T+2T_r)}{(T+\Phi_i)(T+\Phi_i+T_r)},$$

$$J_{LIT,p}(T) = \frac{1.9\times10^4\cdot P(T)^{-2.78}}{1+0.4866P(T)^{-2.51}},$$

[Burger et al., 2000; *Usoskin.,* 2013]

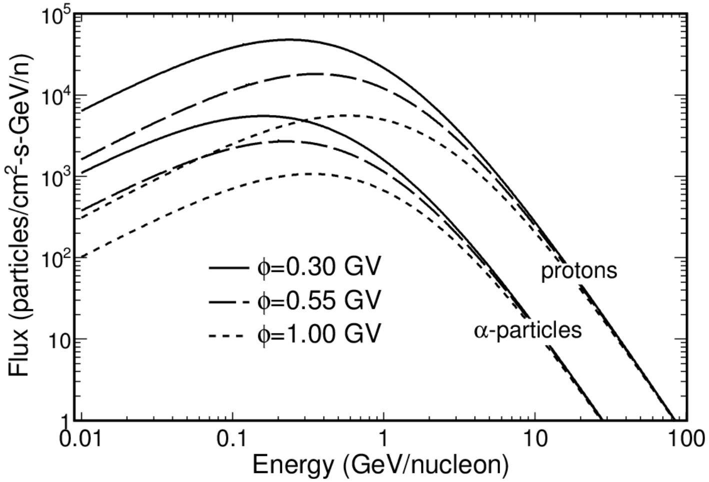

The energy spectra of proton fluxes and α particles fluxes of GCRs with different modulation parameters

J: differential intensity of the flux [particles/ (cm^2 sr s GeV/nucleon)]
T :kinetic energy per nucleon [GeV/nucleon]
$J_{LIT,p}$: the local interstellar spectrum.

$\Phi_i = (Z_i e/A_i)\phi$, ϕ *is the* solar modulation potential [MV],
In our model: ϕ =0.55 GV
At this time, the integral (0.01–100 GeV/nucleon) 4π GCR fluxes of the proton and alpha particles are 3.498 and 0.339 per cm^2 per second, respectively.

- The particle source (SCR particles) :

$$\frac{dJ}{dR} = k\, e^{\frac{R}{R_0}},$$

[Nishiizumi et al., 2009; Reedy and Arnold, 1972]

$$\frac{dJ}{dE_p} = g\, \frac{E_p + m_p c^2}{(E_p^2 + 2m_p c^2 E_p)^{0.5}} e^{\frac{(E_p^2+2m_p c^2 E_p)^{0.5}}{R_0}},$$

J: the flux of SCR,
R: the rigidity (*pc/Ze*) of the particles,
R_0:is a spectral shape parameter[MV], k: is a constant.

The average value R_0 = 80 MV during the last 5 solar cycles (1954 – 2008), and 4π flux *J* (E_p > 10 MeV) = 134 $cm^{-2} s^{-1}$ at 1 AU from the Sun and gave. *Reedy* [2012]

- # Results

1. The flux of neutrons, protons, π^+, π^- in the lunar sample calculated by Geant4

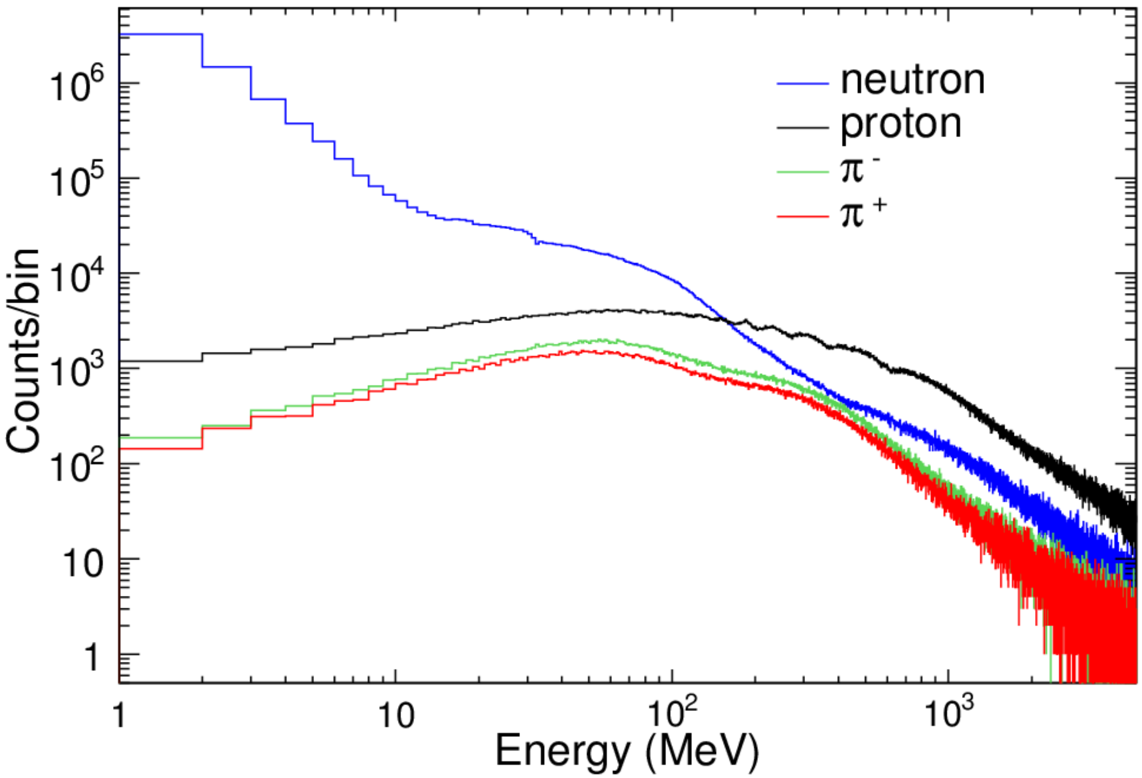

2. The cross-sections of π-nuclear reactions calculated by Geant4.

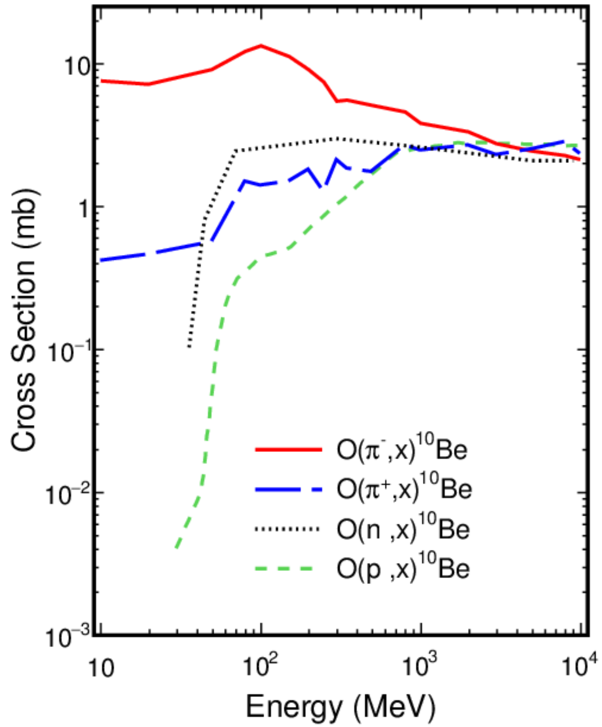

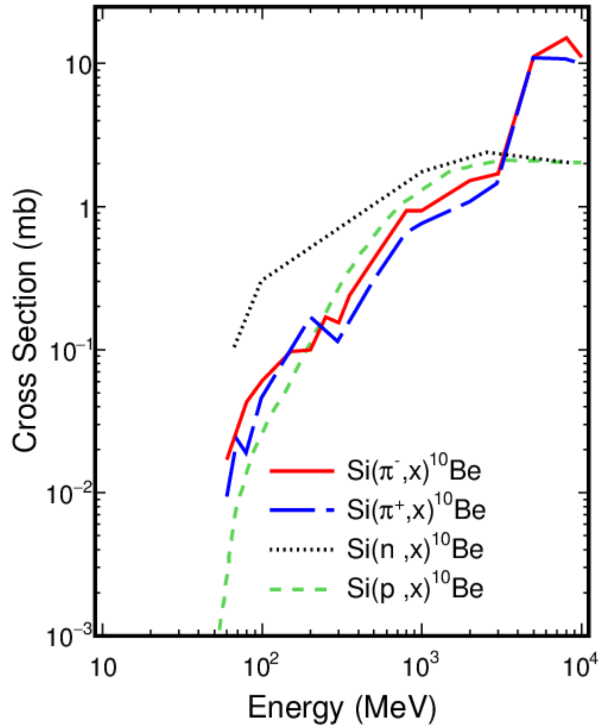

不同反应过程对宇宙成因核素产生率的贡献

Table 2. The contributions of different processes to the production rates of the cosmogenic nuclides. All values are given in percentage.

	(n, x)	(p, x)	(π^-, x)	(π^+, x)	Radioactive Decay	(α, x)	Neutron Capture	else [a]
^{10}Be	56.08	19.94	15.87	5.17	0	1.71	0	1.23
^{14}C	63.36	13.67	13.88	7.48	0.39	0.53	0	0.69
^{26}Al	72.49	14.08	2.72	3.05	6.63	0.46	0	0.57
^{53}Mn	70.36	15.52	1.69	2.32	9.70	0.14	0	0.27
^{36}Cl	83.76	12.18	2.33	1.07	0	0.35	0	0.31
^{41}Ca	0.64	0.51	0.22	0.32	0.03	0.02	98.17	0.09

[a] There are some other processes to produce the cosmogenic nuclides,such as: (K^+, x),(K^0, x), (K^-, x), (^{3}H, x) and (^{3}He, x).

Li, ZHANG et al., JGR 2017

3. The production rates of the cosmogenic nuclides

- ^{53}Mn, ^{41}Ca and ^{36}Cl

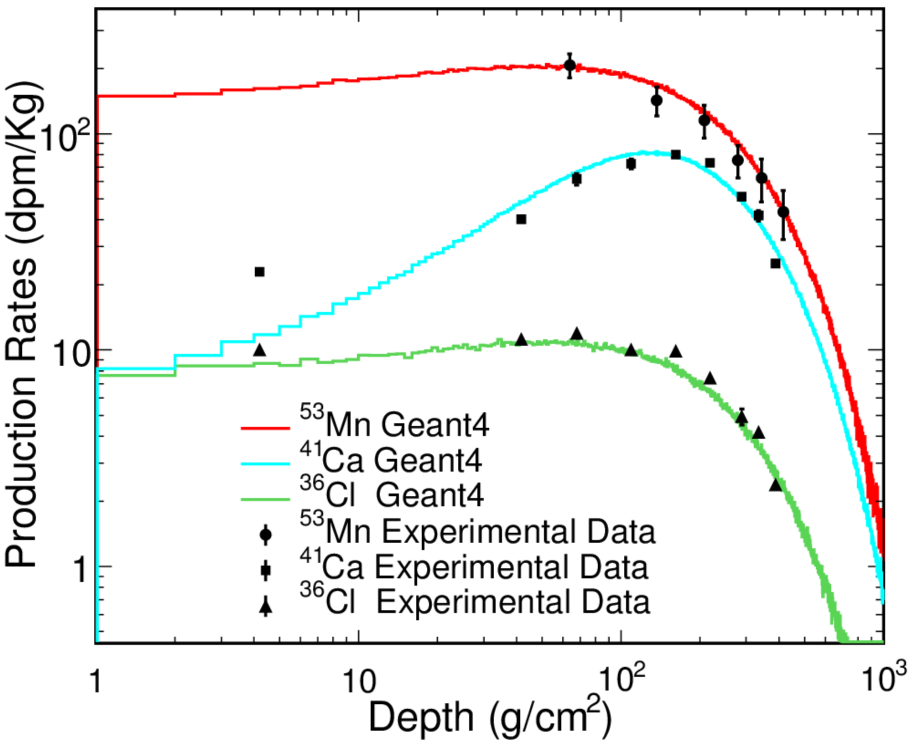

[Imamura and Nishiizumi, 1974; Nishiizumi et al., 1984a, 1997]

The simulation results and the experimental data of the production rates of ^{53}Mn, ^{41}Ca and ^{36}Cl in Apollo 15 Drill Core

➢ ^{26}Al （反应截面优化）

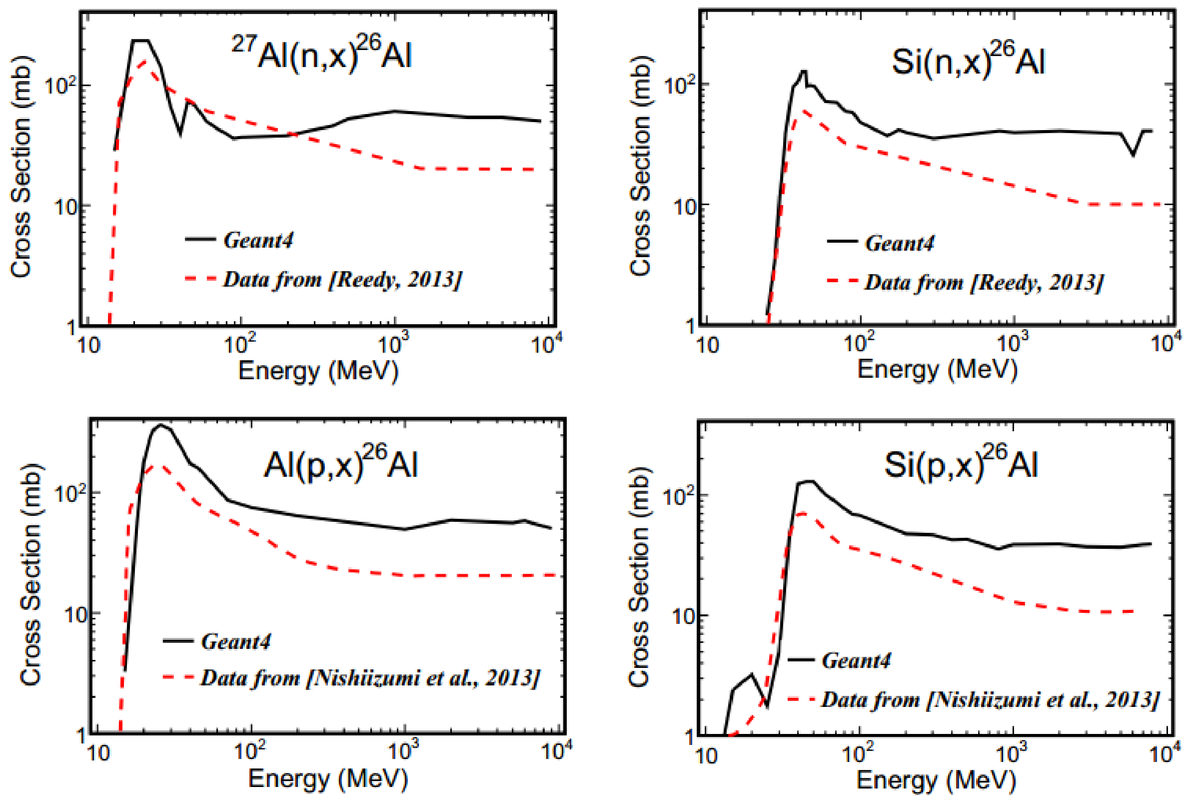

The excitation functions of the reactions

^{27}Al (n, x) ^{26}Al, Si (n, x) ^{26}Al, Al (p, x) ^{26}Al and Si (p,x) ^{26}Al.

- ➢ ^{26}Al

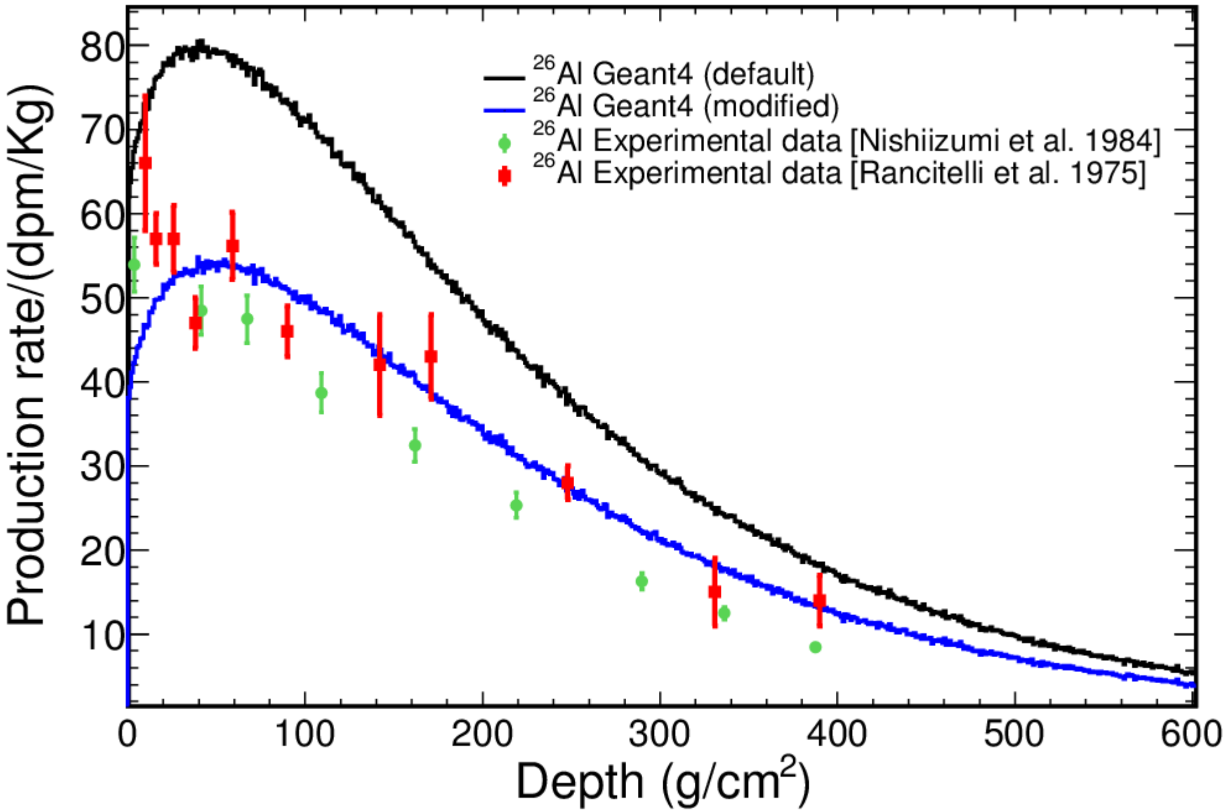

The simulation results and the experimental data of the production rates of ^{26}Al in Apollo 15 Drill Core

➢ ^{14}C and ^{10}Be

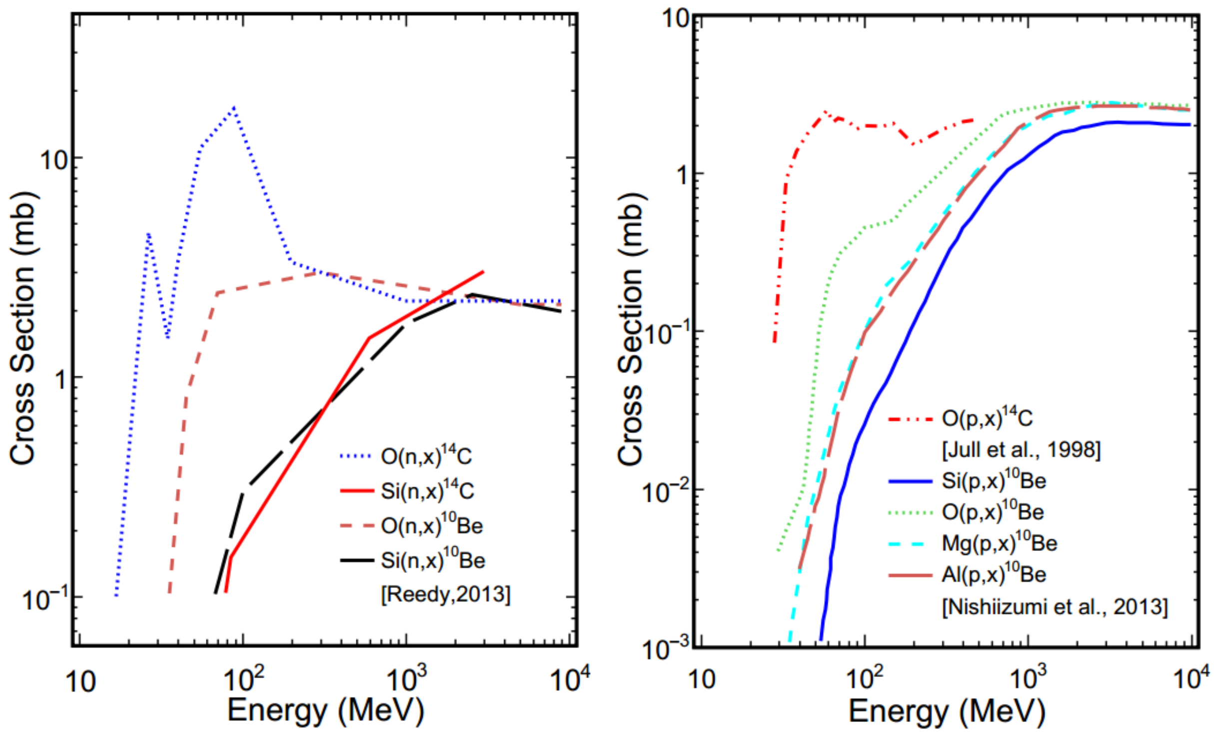

The excitation functions of the reactions O (n, x) ^{14}C, Si (n, x) ^{14}C, O(p, x) ^{14}C, O (n, x) ^{10}Be, Si (n, x) ^{10}Be, O (p, x) ^{10}Be, Mg (p, x) ^{10}Be, Al (p, x) ^{10}Be and Si (p, x) ^{10}Be

➢ ^{14}C and ^{10}Be

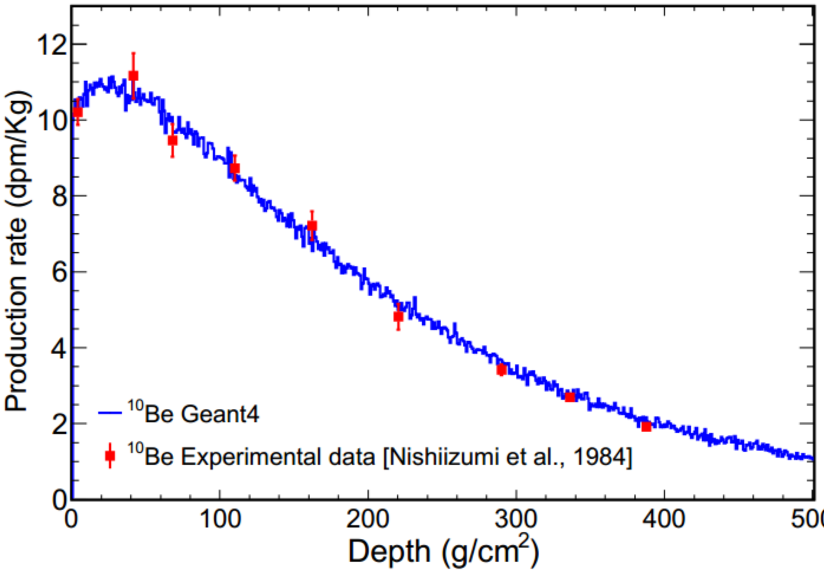

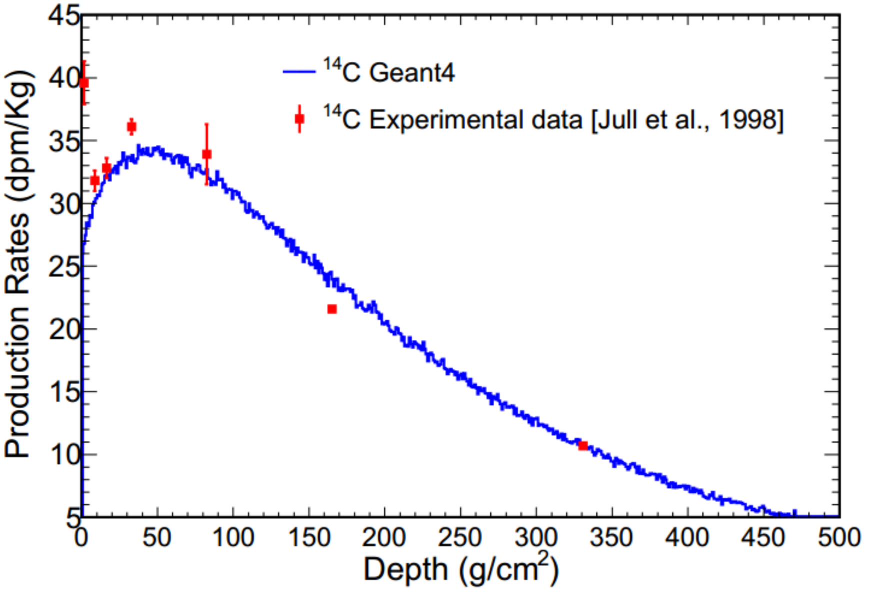

The simulation results and measured data of the production rates of ^{10}Be and ^{14}C

➢ The sum effects of GCR and SCR.

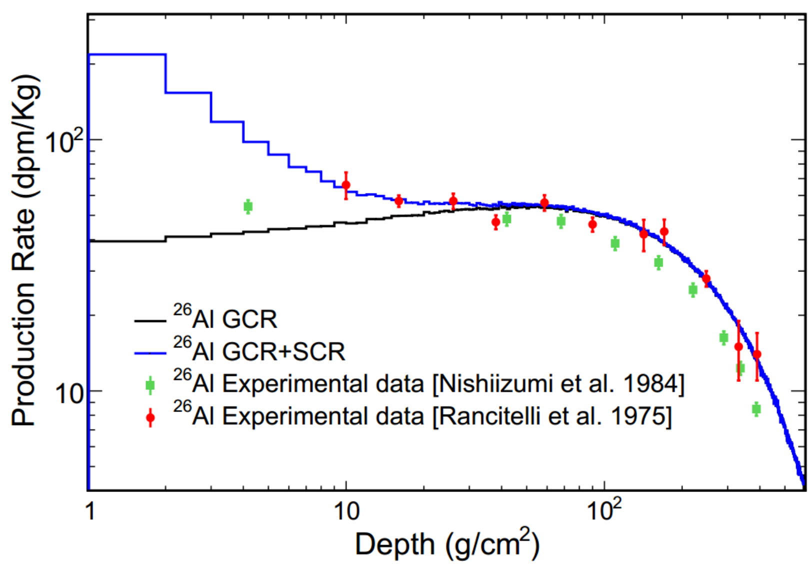

The simulation results of the total ^{26}Al production rates from GCRs and SCRs reactions and the measured data

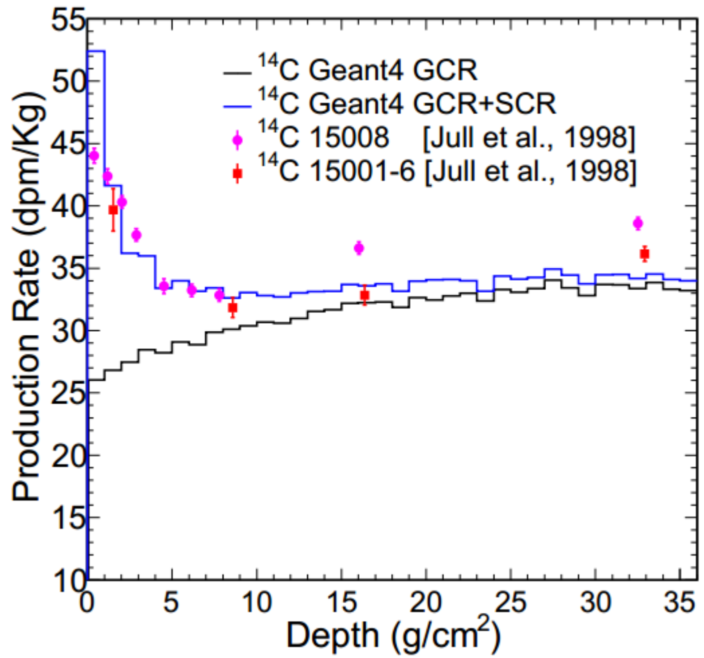

The simulation results of the total ^{14}C production rates from GCRs and SCRs reactions and the measured data

Progress in Particle and Nuclear Physics 109 (2019) 103711

Contents lists available at ScienceDirect

Progress in Particle and Nuclear Physics

journal homepage: www.elsevier.com/locate/ppnp

Review

Spallation, cosmic rays, meteorites, and planetology

J.-C. David [a,*], I. Leya [b]

[a] IRFU, CEA, Université Paris-Saclay, F-91191, Gif-sur-Yvette, France
[b] Physics Institute, University of Bern, Sidlerstrasse 5, 3012 Bern, Switzerland

interest. All were implemented into the INCL4.6 code (and so INCL++) as described in detail in [123,348,394]. It has been shown that it is now possible to reliably calculate contributions from α-induced reactions.

When the incident energy increases, not only the number of secondary π's increases but also their kinetic energies, resulting in higher cosmogenic production rates due to the π's. This topic has recently been investigated by Li et al. [395] using simulations of cosmogenic nuclides on the Moon, calculated using the Geant4 transport code. The secondary π-spectra never exceeded 5 GeV, therefore the Bertini model was used for the π's and the BIC code treated the nucleons. The results for ^{10}Be and ^{14}C were surprising, about 20% of their production comes from π's! For ^{26}Al, ^{36}Cl, and ^{53}Mn the contributions are $\sim$5%. Though, this is within the range of typical uncertainties, it is nevertheless important for studies on model reliabilities and uncertainties. Although some uncertainties still exist, it is obvious that π's can play an important role for cosmogenic nuclide studies. On the same topic, some particular reactions induced by energetic neutrons must be considered very carefully. As previously discussed, major efforts have been done determining the neutron-induced production cross sections. Since few measurements are available, the method developed in [56], i.e., unfolding thick target

A&A 618, A96 (2018)
https://doi.org/10.1051/0004-6361/201833561

Astronomy & Astrophysics

Solar energetic particles and galactic cosmic rays over millions of years as inferred from data on cosmogenic ^{26}Al in lunar samples

S. Poluianov[1,2], G. A. Kovaltsov[3], and I. G. Usoskin[1,2]

been brought to the Earth and measured for the nuclide content and its depth distribution. Estimates of the energetic particle intensity have been conducted earlier [e.g., 1, 2, 3, 4] via quantitative modelling of nuclide production by galactic cosmic rays (GCR) and SEP. Since most of results were obtained decades ago and the quality of modelling of the cosmic ray cascade has increased significantly, the study of cosmogenic nuclide need a revision. Moreover, earlier works considered production of nuclides only by secondary protons, neutrons and α-particles, though Li et al. [5] have shown that the contribution by secondary charged pions cannot be neglected.

minus crossing the depth layers from 0 to 950 g/cm^2 distributed with quasilogarithmic steps from 0.01 to 50 g/cm^2 from top to bottom. We included production of ^{26}Al by pions because their contribution is not negligible in dense matter, as noted by Li et al. [5]. The cross-sections of pion reactions were obtained by direct simulations with GEANT4. The method of computation of the

Conclusions

- The solar modulation of GCR and ACR flux/spectra are studied using the near-Earth satellite or Chang'E-4 LND.
- A numerical simulation model is built based on Geant4 to simulate the production of cosmogenic nuclides. Some modifications have been made for cross sections in Geant4 using the experimental data or other proper model and the contributions of all secondary particles caused by cosmic rays are included in our simulation model.
- Our simulation results suggest a substantial contribution of the secondary charged pions to the production rates of ^{10}Be and ^{14}C, as high as 21.04% for ^{10}Be and 21.36% for ^{14}C, respectively.
- Within one set of self-consistent parameters, the simulation results of the production rates of the cosmogenic nuclides, ^{53}Mn, ^{36}Cl, ^{41}Ca, ^{26}Al, ^{10}Be and ^{14}C, agree well with the measured data from Apollo 15 drill core.
- Outlook: the cosmogenic isotopes could be used for exposure age determination.

Outlook

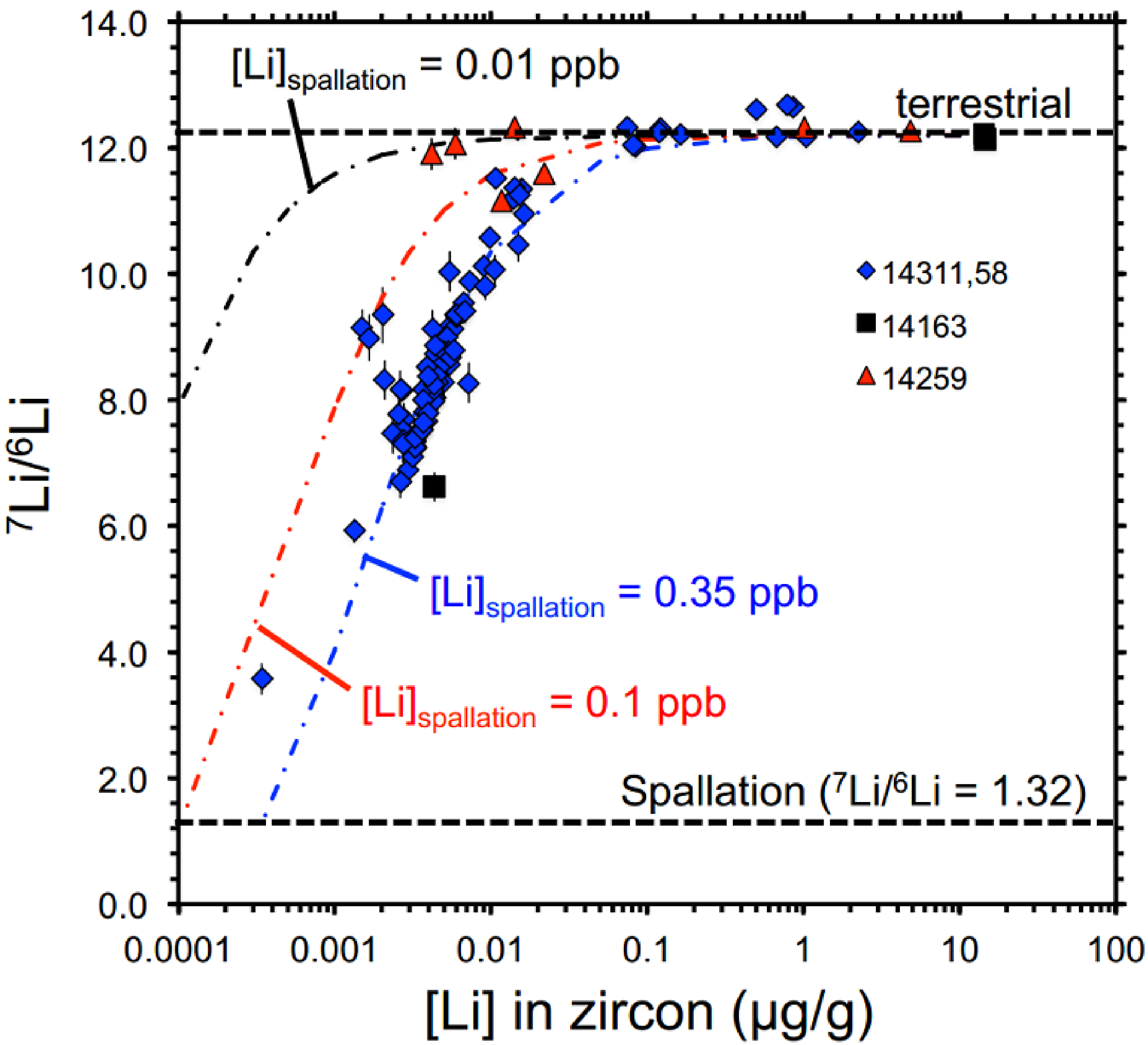

[Li]$_{spallation}$ = 0.01 ppb
terrestrial
14311,58
14163
14259
[Li]$_{spallation}$ = 0.35 ppb
[Li]$_{spallation}$ = 0.1 ppb
Spallation ($^7Li/^6Li$ = 1.32)
$^7Li/^6Li$
14.0
12.0
10.0
8.0
6.0
4.0
2.0
0.0
0.0001
0.001
0.01
0.1
1
10
100
[Li] in zircon (μg/g)

Thank You!